Infectious Disease Modelling 7 (2022) 82–108

Contents lists available at ScienceDirect

Infectious Disease Modelling

journal homepage: www.keaipublishing.com/idm

Optimal control analysis of hepatocytic-erythrocytic dynamics of *Plasmodium falciparum* malaria

Titus Okello Orwa*, Rachel Waema Mbogo, Livingstone Serwadda Luboobi

Institute of Mathematical Sciences, Strathmore University, P.O Box 59 857-00 200, Nairobi, Kenya

ARTICLE INFO

Article history:
Received 17 June 2021
Received in revised form 29 November 2021
Accepted 29 November 2021
Available online 8 December 2021
Handling editor: Dr Y. Shao

Keywords:
Optimal control
Blood schizontocide
Gametocytocide
P. falciparum malaria
Malaria vaccines
Pontryagin's Maximum Principle

ABSTRACT

This paper presents an in-host malaria model subject to anti-malarial drug treatment and malaria vaccine antigens combinations. Pontryagin's Maximum Principle is applied to establish optimal control strategies against infected erythrocytes, infected hepatocytes and malaria parasites. Results from numerical simulation reveal that a combination of pre-erythrocytic vaccine antigen, blood schizontocide and gametocytocide drugs would offer the best strategy to eradicate clinical *P. falciparum* malaria. Sensitivity analysis, further reveal that the efficacy of blood schizontocides and blood stage vaccines are crucial in the control of clinical malaria infection. Futhermore, we found that an effective blood schizontocide should be used alongside efficacious blood stage vaccine for rapid eradication of infective malaria parasites. The authors hope that the results of this study will help accelerate malaria elimination efforts by combining malaria vaccines and anti-malarial drugs against the deadly *P. falciparum* malaria.

© 2021 The Authors. Publishing services by Elsevier B.V. on behalf of KeAi Communications Co. Ltd. This is an open access article under the CC BY-NC-ND license (http://creativecommons.org/licenses/by-nc-nd/4.0/).

1. Introduction

Malaria is a major leading public health problem, especially in the African continent (Aguilar & Gutierrez, 2020; Yiga, Nampala, & Tumwiine, 2020). In 2019, about 229 million cases and 409 000 deaths due to malaria infections were reported globally (Al-Awadhi, Ahmad, & Iqbal, 2021; WHO, 2020). The (WHO)African Region bore the heaviest burden, accounting for 94% of all reported global malaria cases and deaths in 2019. Existing control measures and treatment therapies have lead to a 1.5 billion and 7.6 million averted malaria cases and malaria-related deaths, respectively, since the year 2000 (WHO, 2020). However, the 2020 world malaria report showed an increase in case incidence in some high burden countries in Africa and Americas (WHO, 2020). Currently, treatment using antimalarial drugs is the main control available for clinical malaria infections (Orwa et al., 2019a). Moreover, artemisinin-based combination therapy (ACT) is the standard of care for uncomplicated *P. falciparum* malaria worldwide (Arya, Foko, Chaudhry, & Singh, 2020) . Drug resistance against 4-aminoquinolines and sulpha compounds has remained one of the greatest challenge to malaria chemotherapy development (Visser, van Vugt, & Grobusch, 2014). Further evidence of resistance to artemisinins (Dondorp et al., 2009; Noedl et al., 2008) highlights the need for continuous investment in alternative anti-malarial drugs and malaria vaccines.

* Corresponding author.
E-mail address: torwa@strathmore.edu (T.O. Orwa).
Peer review under responsibility of KeAi Communications Co., Ltd.

https://doi.org/10.1016/j.idm.2021.11.006
2468-0427/© 2021 The Authors. Publishing services by Elsevier B.V. on behalf of KeAi Communications Co. Ltd. This is an open access article under the CC BY-NC-ND license (http://creativecommons.org/licenses/by-nc-nd/4.0/).

Combination of anti-malarial drugs have achieved tremendous success in malaria treatment and transmission reduction (NIH, 2019; Visser et al., 2014). Administration of at least two anti-malarial drug regimens with different modes of action and target has been shown to be highly effective compared to monotherapy drugs (WHO, 2015a). A rapidly acting artemisinin drug in ACTs exhibit an extremely short half-life. It is hence combined with a longer-acting monotherapy drug to limit recrudescence and achieve higher clinical response (WHO, 2018). The artemisinin component reduces malaria parasite density by a factor of about 10^4 within 2 days of asexual cycle (Hodel, Kay, & Hastings, 2016). Furthermore, it is active against blood floating gametocytes that are responsible for infection transmission to mosquito vector. The monotherapy drug with a longer half-life eradicates the rest of the parasites that are not cleared by the artemisinin drug. This further reduces the possible occurrence of resistance due to mutations during treatment. Additionally, the long-acting drug may provide prophylaxis after treatment (WHO, 2015b). In (Okell, Drakeley, Bousema, Whitty, & Ghani, 2008), a combination of an ACT partner drug and a nonartemisinin regimen is shown to have a greater impact in higher-transmission settings. The combination of artesunate and amodiaquine reduced gametocyte density and showed minimal effect on tolerability in *P. falciparum* patients (Osorio, Gonzalez, Olliaro, & Taylor, 2007). Elsewhere (Smithuis et al., 2010), a combination of artesunate and mefloquine greatly suppressed malaria in Myanmar.

Although malaria drugs and insecticides have helped reduce malaria cases and deaths globally, these two in-host malaria control measures are vulnerable to parasite development of resistance (Chitnis et al., 2015; Duru, Witkowski, & Ménard, 2016). Evidence of *P. falciparum* resistance to artesunate in Western Cambodia was characterized by slow parasite clearance (Dondorp et al., 2009; Mairet-Khedim et al., 2020). Efficacious malaria vaccine is likely to fill malaria elimination gap (Abdulla et al., 2011; Orwa et al., 2019b). Unfortunately, malaria vaccine development has been impeded by the complex biology of malaria parasites and the many parasites infection cycles (Mahmoudi & Keshavarz, 2018). Several clinical and preclinical studies (Bauza, Atcheson, Malinauskas, Blagborough, & Reyes-Sandoval, 2016; Mahmoudi & Keshavarz, 2018; Sherrard-Smith et al., 2018) have demonstrated the significant benefit of combining two or more malaria vaccine antigens. A combination of recombinant PfMSP-1_{42} and AS02A induced high concentrations of antibody among young children in Western Kenya (Ogutu et al., 2009). In (Chitnis et al., 2015), JAIVAC-1 and Montanide ISA720 induced proportional antibody responses against PfF2 and PfMSP-1_{19}.

In developing response plans to malaria infections, decision makers such as government and public health officers are often faced with trade-offs in choosing among various malaria treatment and control options (Gaff & Schaefer, 2009). The usual challenge, however, is to find the optimal response balancing treatment and vaccination that will minimize incidence and disease-related mortality at an affordable cost (Joshi, Lenhart, Li, & Wang, 2006; Omondi, Orwa, & Nyabadza, 2018). Optimal control theory (Lenhart & Workman, 2007) has been very helpful in identifying optimal control measures against particular diseases. In malaria epidemiology, the application of optimal control theory has for a long time been limited to population level models (Agusto, Marcus, & Okosun, 2012; Makinde & Okosun, 2011; Mwanga, Haario, & Capasso, 2015; Okosun, Ouifki, & Marcus, 2011). In most of these models, the main objective has been to minimize the population of malaria-infected humans at a minimal cost (Mwanga et al., 2015).

In (Okosun et al., 2011), a combination of vaccination and treatment methods is shown to be the optimal control strategy against malaria infection at population level. Moreover, a combination of screening, treatment and use of insecticidals is shown to be highly effective against malaria infections and transmissions among susceptible immigrants (Makinde & Okosun, 2011). In (Silva & Torres, 2013), optimal supervision and educational campaigns on the use of insecticide treated nets (ITNs) are shown to be highly effective in achieving 75% coverage of the host population within a community. Analysis in (Mwanga, Haario, & Nannyonga, 2014), reveal that a combination of three malaria controls: ITNs, indoor residual spraying (IRS) and drug treatment provides the best control measure against malaria transmission and infection within a community. Additionally, control targeting mosquito vector is more effective than personal protection in some cases but not always (Kim et al., 2012). In (Agusto et al., 2012), a combination of insecticides, antimalarial drugs and personal protection are shown to bear the greatest impact on malaria control. In all these dynamical models, optimal control strategies were established based on Pontryagin's Maximum Principle (PMP) (Anita, Capasso, & Arnautu, 2011).

In (Orwa et al., 2018b), a combination of different vaccine antigens are shown to greatly reduce parasitemia and severity of *P. falciparum* malaria infection. Additionally, a combination of two malaria drugs, fosmidomycin and piperaquine was also established to have higher efficacy, safety and well tolerated (Mombo-Ngoma et al., 2017). Elsewhere (Pukrittayakamee et al., 2004), a combination of artesunate and primaquine resulted in significantly shorter gametocyte clearance times. Although artesunate inhibits gametocyte development, the partner drug, primaquine, is shown to accelerates gametocyte clearance in (Pukrittayakamee et al., 2004). In this paper, we argue that a combination of efficient antimalarial drugs and efficacious malaria vaccines present the best therapeutic strategy to achieving malaria elimination. The theory of optimal control is applied to an in-host malarial model that is characterized by a combination of antimalarial drugs and different vaccine antigens. To the best of our knowledge, this study is the first of its kind to apply optimal control theory to an in-host malaria model with therapeutic control measures. The objective of the paper is to establish an optimal combination therapy for clinical *P. falciparum* malaria.

The rest of the paper is organized as follows. The in-host malaria model with time-dependent antimalarial drug therapy and malaria vaccine controls is presented in Section 2. Analysis of the model with constant controls is presented in Section 3. The formulation of optimal control problem and the proof of existence and uniqueness of solutions of the optimality system is provided in Section 4. Sensitivity analysis is also performed in Section 4. In Section 5, the optimality system is solved

numerically, using the backward-forward sweep algorithm and the 4th order Runge-Kutta scheme in Matlab. This study is finally concluded in Section 6.

2. Mathematical model

An in-host *P. falciparum* malaria model is formulated to study optimal malaria control strategies within the human host. The deterministic model is an extension of the model in (Orwa et al., 2018a) and comprises of nine compartments of: (i) sporozoites (S), (ii) uninfected hepatocytes (H), (iii) infected hepatocytes (X), (iv) uninfected red blood cells (R), (v) early stage infected red blood cells (blood trophozoites, T), (vi) mature infected red blood cells (blood schizonts, C), (vii) merozoites (M), (viii) gametocytes (G) and (ix) $CD8^+$ T cells (Z). The in-host malaria is subjected to a combination of malaria vaccine and anti-malarial drug control strategies. The specific vaccines are: RTS,S/AS01 (a pre-erythrocytic vaccine) (Birkett, 2016)) and merozoite surface protein 3 (MSP3) (blood stage vaccines) (Miura, 2016), which offer direct protection to the human-host. The antimalarial drugs considered here are artemether-lumefantrine (AL) (a blood schizontocide) (Ogutu, 2013)) and primaquine (PQ) (a gametocytocide) (WHO, 2012)). The combined chemotherapy not only target rapid parasite clearance but also reduced parasite transmissibility to mosquito vector. Note that the four malaria control measures considered in this paper, target different sites within the complex malaria parasite life cycle (CDC, 2017) within the human host.

The recruitment of the hepatocytes is assumed to occur at the rate λ_h through self-replication. Sporozoite invasion at the rate β_s results in the formation of infected hepatocytes X. A mature liver schizont burst open to release N merozoites into the blood stream. This marks the start of the erythrocytic cycle. Healthy red blood cells (erythrocytes) are recruited at the rate λ_r from the bone marrow. Merozoite invasion of the uninfected red blood cells at a rate β_r is a complex and ordered process (Cowman, Berry, & Baum, 2012). The infected red blood cells T mature at the rate γ into blood schizonts C that rupture to release more merozoites into blood stream. A proportion π of asexual merozoites commit to form sexual gametocytes G. Human defensive immune cells play a critical role during pathogen invasion. The $CD8^+$ T cells are recruited at a constant rate λ_z from the thymus. The production of $CD8^+$ T cells is furthermore aggravated by the presence of infected hepatocytes, blood trophozoites and blood schizonts at the rates δ_x, δ_t and δ_c, respectively. Therefore, (δ_x, δ_t, δ_c) represents the immunogenicity of the state variables X, T and C, respectively. The limiting effects of $CD8^+$ T cells during parasite invasion is described using a nonlinear bounded Michaelis-Menten-Monod function (Orwa et al., 2018b). The parameters μ_s, μ_m, μ_g represents the death rates of sporozoites, merozoites and gametocytes respective.

The in-host malaria model is further subjected to a combination of malaria vaccine and anti-malarial drug control strategies. These control measures reduce the rates of parasite invasions at the liver and blood stages, respectively. The specific vaccines under our consideration are: (1) RTS,S/AS01 (a pre-erythrocytic vaccine) (Birkett, 2016)) and (2) merozoite surface protein 3 (MSP3) (blood stage vaccines) (Miura, 2016). We also consider two antimalarial drugs (2) artemether-lumefantrine (a blood schizontocide) (Ogutu, 2013)) and (3) primaquine (a gametocytocide) (WHO, 2012)). The combined chemotherapy not only target rapid parasite clearance but also reduced parasite transmissibility to mosquito vector. The gametocytocide considered in this study is a single dose 0.25 mg base/kg of primaquine. This WHO recommended drug (Eziefula et al., 2014; Pukrittayakamee et al., 2004; White, Qiao, Qi, & Luzzatto, 2012; WHO, 2012), mainly targets the blood stage gametocytes. This reduces the probability of parasite transmission to the mosquito vector and hence disease morbidity.

The Pontryagin's Maximum Principle is applied to minimize the population of infected hepatocytes, infected erythrocytes, infective blood stage merozoites and the gametocytes. MSP3 and RTS,S/AS01 reduces the rates of invasion of healthy

Table 1
Description of model parameters.

Parameter	Description
μ_s	Death rate of sporozoites
Λ	The rate of injection of sporozoites into liver due to mosquito bites
β_s	Rate of invasion of hepatocytes by sporozoites
λ_h	Rate of supply of hepatocytes from the bone marrow
λ_r	Rate of supply of erythrocytes from the bone marrow
μ_h, μ_x	Death rate of susceptible hepatocyte and infected hepatocyte, respectively
π	Proportion of parasites that become gametocytes per bursting blood schizont C
k_x, k_t, k_c	Immunosensitivity of X, T and C, respectively
δ_x, δ_t, δ_c	Immunogenecity of X, T and C, respectively
μ_r	Natural mortality rate of healthy RBC
β_r	Rate of infection of RBCs by merozoites
μ_t, μ_c	Rate of decay of blood trophozoites and blood schizonts, respectively
μ_m, μ_g	Rate of decay of merozoites and gametocytes, respectively
P	Average number of merozoites released per bursting blood schizont
N	The average number of merozoites released per bursting infected hepatocytes
γ	Rate of progression from blood trophozoite to schizont stages
α	Rate of inhibition of immune response
λ_z	Rate of production of $CD8^+$ T-cells
$1/\epsilon_0$, $1/\epsilon_1$, $1/\epsilon_2$	Half saturation constants for X, T and C, respectively
μ_z	Rate of decay of $CD8^+$ T-cells

hepatocytes and healthy erythrocytes, respectively. The hepatocyte invasion rate β_s and the erythrocyte invasion rates β_r are hence, reduced to $(1-u_1(t))\beta_s$ and $(1-u_2(t))\beta_r$, respectively. The time dependent controls $u_1(t)$ and $u_2(t)$, therefore represents the efficacies of the pre-erythrocytic vaccine and the blood stage vaccine, respectively. The administration of AL, reduces the average number of merozoites released per bursting blood schizont P to $(1-u_4(t))P$, where $u_4(t)$ is the normalized AL dosage efficacy as a function of time (MA, 2019). Similarly, the use of primaquine reduces the average number of merozoites released per bursting infected hepatocyte N to $(1-u_3(t))N$, where $u_3(t)$ is the normalized primaquine dosage efficacy as a function of time. Based on these additional assumptions and model dynamics, we have the following optimal control model for in-host *P. falciparum* malaria:

$$\left.\begin{aligned}
\frac{dS}{dt} &= \Lambda - \mu_s S - \beta_s SH,\\
\frac{dH}{dt} &= \lambda_h - \mu_h H - (1-u_1(t))\beta_s SH,\\
\frac{dX}{dt} &= (1-u_1(t))\beta_s SH - \mu_x X - \frac{k_{xZX}}{1+\epsilon_0 X},\\
\frac{dR}{dt} &= \lambda_r - \frac{(1-u_2(t))\beta_r RM}{1+\alpha Z} - \mu_r R,\\
\frac{dT}{dt} &= \frac{(1-u_2(t))\beta_{rRM}}{1+\alpha Z} - \mu_t T - \gamma T - \frac{k_{tZT}}{1+\epsilon_1 T},\\
\frac{dC}{dt} &= \gamma T - \mu_c C - \frac{k_c ZC}{1+\epsilon_2 C},\\
\frac{dM}{dt} &= (1-u_3(t))N\mu_x X + \frac{(1-u_4(t))P(1-\pi)\mu_c C}{1+\alpha Z} - \mu_m M - \beta_r RM,\\
\frac{dG}{dt} &= \pi\mu_c C - (u_3(t)+\mu_g)G,\\
\frac{dZ}{dt} &= \lambda_z + Z\left(\frac{\delta_x X}{1+\epsilon_0 X} + \frac{\delta_t T}{1+\epsilon_1 T} + \frac{\delta_c C}{1+\epsilon_2 C}\right) - \mu_Z Z.
\end{aligned}\right\}, \tag{1}$$

subject to the initial conditions: $S(0)\geq 0$, $H(0)>0$, $X(0)\geq 0$, $R(0)>0$, $T(0)\geq 0$, $C(0)\geq 0$, $M(0)\geq 0$, $G(0)\geq 0$, $Z(0)>0$.

A brief description of model parameters are presented in Table 1.

2.1. Well-posedness of the model

The optimal system (1) is epidemiologically meaningful if all its solutions with non-negative initial conditions remain non-negative for all time $t\geq 0$.

Theorem 1. *If the initial values $S(0)$, $H(0)$, $X(0)$, $R(0)$, $T(0)$, $C(0)$, $M(0)$, $G(0)$ and $Z(0)$ are non-negative, then the solution $(S(t), H(t), X(t), R(t), T(t), C(t), M(t), G(t), Z(t))$ of system (1) is non-negative for all time $t\geq 0$.*

Additionally, based on the Theorem by Garrett Birkhoff and Gian-Carlo Rota (Garrett & Rota, 1978), we have

$$N_e(t)\leq \max\left\{N_e(0), \tfrac{\lambda_r}{\mu_e}\right\}, N_l(t)\leq \max\left\{N_l(0), \tfrac{\lambda_h}{\mu_l}\right\}, N_p(t)\leq \max\left\{N_p(0), \tfrac{(\Lambda}{\mu_p}\right\},$$
$$Z(t)\leq \max\left\{Z(0), \tfrac{\lambda_z}{\mu_z}\right\},$$

where $N_e(t)=R(t)+T(t)+C(t)$, $N_l(t)=H(t)+X(t)$, $N_p(t)=S(t)+M(t)+G(t)$, $\mu_e=\min\{\mu_r, \mu_t, \mu_c\}$, $\mu_l=\min\{\mu_h, \mu_x\}$ and $\mu_p=\min\{\mu_s, \mu_m, \mu_g\}$.

Furthermore, the region of biological relerance Φ is given by

$$\begin{aligned}\Phi = \Big\{(S,H,X,R,T,C,M,G,Z)\in\mathbb{R}_+^9 : N_e(t)\leq \max\left\{N_e(0), \frac{\lambda_r}{\mu_e}\right\}, N_l(t)\leq \max\left\{N_l(0), \frac{\lambda_h}{\mu_l}\right\},\\ N_p(t)\leq \max\left\{N_p(0), \frac{\Lambda}{\mu_p}\right\}, Z(t)\leq \max\left\{Z(0), \frac{\lambda_z}{\mu_z}\right\}\Big\}.\end{aligned} \tag{2}$$

We therefore conclude that the set Φ is positively invariant. Thus, all solutions in Φ remain in Φ for all time $t\geq 0$. The optimal system (1) is therefore well-posed mathematically and epidemiologically in the region Φ. It is therefore sufficient to study the dynamics generated by system (1) in Φ. flushleft

3. Analysis of optimal model with constant controls

3.1. Disease-free equilibrium point and effective reproduction number

The optimal system (1) has a disease-free equilibrium state $\mathcal{E}_d$ denoted by

$$\mathcal{E}_d = (S_0, H_0, X_0, R_0, T_0, C_0, M_0, G_0, Z_0) = \left(0, \frac{\lambda_h}{\mu_h}, 0, \frac{\lambda_r}{\mu_r}, 0, 0, 0, 0, \frac{\lambda_z}{\mu_z}\right). \tag{3}$$

At $\mathcal{E}_d$, there are no sporozoite recruitment and the human host is free of malaria parasites (sporozoites, merozoites and gametocytes). To eliminate malaria infection, we apply control measures that would reduce the transmission process and ensure stability of $\mathcal{E}_d$ (Chiyaka, Garira, & Dube, 2008).

The effective reproduction number R_{eff} of the *P. falciparum* malaria is defined as the number of secondary infected erythrocytes generated per primary infected erythrocyte in a human host from the onset of malaria infection (Molineaux & Dietz, 1999) and (Chiyaka et al., 2008). Epidemiologically, if $R_{eff} < 1$, then on average a single infected red blood cell produces less than one new infected red blood cell and the within-host infection cannot grow. Conversely, if $R_{eff} > 1$, then on average, each infected red blood cell generates at least two new infected erythrocytes and parasitaemia is likely to grow leading to severe malaria case.

Using the next generation matrix approach described in (Van den Driessche & Watmough, 2002) and the notations therein, the matrices F and V^{-1} are computed as follows:

$$F = \begin{pmatrix} 0 & 0 & 0 & 0 & 0 & 0 \\ \frac{(1-u_1)\beta_s\lambda_h}{\mu_h} & 0 & 0 & 0 & 0 & 0 \\ 0 & 0 & 0 & 0 & \frac{(1-u_2)\beta_r\lambda_r}{\mu_r} & 0 \\ 0 & 0 & 0 & 0 & 0 & 0 \\ 0 & 0 & 0 & 0 & 0 & 0 \\ 0 & 0 & 0 & 0 & 0 & 0 \end{pmatrix} \tag{4}$$

and

$$V^{-1} = \begin{pmatrix} \frac{\mu_h}{\beta_s\lambda_h + \mu_h\mu_s} & 0 & 0 & 0 & 0 & 0 \\ 0 & \frac{1}{\mu_x} & 0 & 0 & 0 & \\ 0 & 0 & \frac{1}{\gamma+\mu_t} & 0 & 0 & \\ 0 & 0 & \frac{\gamma}{\mu_c(\gamma+\mu_t)} & \frac{1}{\mu_c} & 0 & 0 \\ 0 & \frac{N(1-u_3)\mu_r}{\beta_r\lambda_r+\mu_m\mu_r} & \frac{P(1-\pi)\gamma(1-u_4)\mu_r}{(\beta_r\lambda_r+\mu_m\mu_r)(\gamma+\mu_t)} & \frac{P(1-\pi)\gamma(1-u_4)\mu_r}{(\beta_r\lambda_r+\mu_m\mu_r)} & \frac{\mu_r}{\mu_m\mu_r+\beta_r\lambda_r} & 0 \\ 0 & 0 & \frac{\pi\gamma}{(u_3+\mu_g)(\gamma+\mu_t)} & \frac{\pi}{u_3+\mu_g} & 0 & \frac{1}{u_3+\mu_g} \end{pmatrix} \tag{5}$$

The effective reproduction number is the spectral radius of the next generation matrix (FV^{-1}). Upon computation in Mathematica software, we obtain

$$R_{eff} = \frac{P(1-\pi)(1-u_2)(1-u_4)\gamma\mu_r\beta_r\lambda_r}{(\beta_r\lambda_r+\mu_m\mu_r)(\gamma+\mu_t)}. \tag{6}$$

The following theorem results from the existence of the disease effective reproduction number.

Theorem 2. *The disease-free equilibrium $\mathcal{E}_d$ is locally asymptotically stable when $R_{eff} < 1$ and unstable when $R_{eff} > 1$.*

3.2. Global asymptotic stability of the disease-free equilibrium point

If at any time, using appropriate interventions (such as effective antimalarial drugs and or efficacious malaria vaccines) we are able to reduce R_{eff} to less than unity, then within-host malaria infection may be eliminated.

Theorem 3. *The disease-free equilibrium $\mathcal{E}_d$ of system (1) is globally asymptotically stable if the threshold quantity $R_{eff} < 1$.*
Proof: See Appendix A.flushleft

The above result shows that in-host malaria infection would be eliminated provided that the threshold quantity R_{eff} is less that unity. This is achievable if effective antimalarial drugs are used alongside efficacious malaria vaccines. In-host malaria elimination should hence focus on eradicating infective malaria merozoites and infected erythrocytes.

3.3. Endemic equilibrium point

The stability of the disease-free equilibrium point E_d is violated when $R_{eff} > 1$. System (1) therefore assumes an endemic equilibrium $\mathcal{E}_e$, where

$$\mathcal{E}_e = (S^*, H^*, X^*, R^*, T^*, C^*, M^*, G^*, Z^*). \tag{7}$$

and

$$H^* = \frac{\lambda_h}{\beta_s(1-u_1)S^* + \mu_h}, \quad X^* = \frac{\lambda_h\beta_s(1-u_1)S^*}{(k_xZ^* + \mu_x)(\mu_h + \beta_s(1-u_1)S^*)}, \quad S^* = \frac{b_s + \sqrt{b_s^2 - 4a_sc_s}}{2a_s},$$

$$R^* = \frac{\lambda_r(1+\alpha Z^*)}{M^*(1-u_2)\beta_r + (1+\alpha Z^*)\mu_r}, \quad M^* = \frac{P(1-\pi)(1-u_4)\mu_c + NX^*(1+\alpha Z^*)(1-u_3)\mu_3}{(1+\alpha Z^*)(\beta_rR^* + \mu_m)},$$

$$G^* = \frac{\pi\mu_cC^*}{u_3+\mu_g}, \quad Z^* = \frac{\lambda_z}{\mu_z - \Delta_z}, \quad \text{where} \quad \Delta_z = \frac{\delta_xX^*}{1+\varepsilon_0X^*} + \frac{\delta_tT^*}{1+\varepsilon_1T^*} + \frac{\delta_cC^*}{1+\varepsilon_3C^*},$$

$$T^* = \frac{b_t + \sqrt{b_t^2 - 4a_tc_t}}{-2a_t} \quad \text{and} \quad C^* = \frac{b_c + \sqrt{b_c^2 - 4a_cc_c}}{-2a_c},$$

where

$$a_s = (1-u_1)\beta_s\mu_s > 0, \quad b_s = \beta_s(\lambda_h - \Lambda(1-u_1)) + \mu_h\mu_s, \quad c_s = -\Lambda\mu_h < 0, \tag{8}$$

$$a_t = -(1+\alpha Z^*)\varepsilon_1(\gamma+\mu_t) < 0, \quad b_t = -k_xZ^* + \varepsilon_1\beta_r(1-u_2)M^*R^* - (1+\alpha Z^*)(\gamma+\mu_t), \tag{9}$$

$$a_c = -\varepsilon_2\mu_c < 0, \quad b_c = \gamma\varepsilon_2T - (k_cZ^* + \mu_c), \quad c_c = \gamma T^* \quad \text{and} \quad c_t = (1-u_2)\beta_rM^*R^*. \tag{10}$$

By Descartes' "Rule of Signs" (Wang, 2004), it is clear from the coefficients in equations (8)-(10) that all the state variables would assume a unitary (single) value at the endemic equilibrium point $\mathcal{E}_e$. Effective interventions in the form of antimalarial drugs and efficacious malaria vaccines are necessary to drive the endemic equilibrium state to disease-free state within the human host.

3.4. Sensitivity analysis

Sensitivity analysis is performed to establish the inherent effect on output variables generated by uncertainties in the input parameters (Iooss and Saltelli, 2017). We determine the contribution of vital model parameters to the progression of in-host malaria infection. Using the technique of Latin Hypercube Sampling and Partial Rank Correlation Coefficient (LHS/PRCC) (Iman & Helton, 1988), we establish the model parameters with significant influence in in-host malaria disease dynamics. Using 1000 simulations per run and parameter baseline values provided in Tabe 2, we determined the PRCCs of the parameters in the disease reproduction number R_{eff} in equation (6). Results of sensitivity analysis are presented in Fig. 1. Note that parameters with positive (or negative) PRCC increases (or decreases) the disease R_{eff} when they are increased (or decreased). Subsequently, this increases (or decreases) the levels of parasitaemia within infected human host. Observe that (i) the death rate of blood trophozoites μ_t, (ii) the rate of progression of trophozoites to blood schizont stages γ, (iii) efficacy of blood stage vaccine μ_2 and (iv) efficacy of blood schizontocide μ_4, are the four influential parameters in driving the in-host malaria dynamics. It is further evident that μ_2 and μ_4 are the most sensitive parameters in model system (1). The disease dynamics is hence heavily influenced by the efficacy antimalarial drugs that target blood trophozoites and blood schizonts.

4. Formulation of optimal control problem

We endevour to reduce malaria disease severity within the human host by reducing parasite invasion of the healthy hepatocytes and erythrocytes. To curtail further transmission, we also aim to reduce the density of sexual gametocytes within the host's blood stream. To achieve these two, we set out to establish the most-effective control strategy drawn from a combination of malaria vaccine antigens and antimalarial drugs regimens described in Section 2. The malaria control measures/strategies under our consideration are $u_1(t)$, $u_2(t)$, $u_3(t)$ and $u_4(t)$ described in Section 2. Therefore, the objective functional J defined over the controls $(u_1, \ldots, u_4)$ and within a finite time interval $[0, t_f]$ is given by

$$J(u_1, \ldots, u_4) = \int_0^{t_f} (A_1X + A_2T + A_3M + A_4G) + \frac{1}{2}\sum_{i=1}^{4} B_i u_i^2, \tag{11}$$

subject to the differential system (1).

In equation (11), $A_1, \ldots, A_4$ are the costs associated with minimising the infected hepatocyte, infected erythrocytes, the merozoites and gametocytes, respectively. The parameter t_f denotes the time period of intervention. The quantities $B_1, \ldots, B_4$ represents the weight constants for pre-erythrocytic vaccine, blood stage vaccine, blood schizontocide and gametocytocide, respectively. Additionally, we endevour to minimize the costs associated with the control efforts: pre-erythrocytic vaccines $\frac{1}{2}B_1u_1^2$, blood stage vaccine $\frac{1}{2}B_2u_2^2$, blood schizontocide $\frac{1}{2}B_3u_3^2$ and gametocytocide $\frac{1}{2}B_4u_4^2$.

Like other disease models (Joshi et al., 2006; Okosun et al., 2011), the costs associated with using antimalarial drugs and malaria vaccines are directly proportional to the rates of implementation of these control measures. Therefore, the coefficients A_1X, A_2T, A_3M and A_4G are linear functions. On the other hand, the cost of administering the listed control measures, $\frac{1}{2}B_1u_1^2$, $\frac{1}{2}B_2u_2^2$, $\frac{1}{2}B_3u_3^2$ and $\frac{1}{2}B_4u_4^2$ are directly proportional to the square of the corresponding control function. They are hence nonlinear and take quadratic forms.

Numerically, we endevour to establish an optimal control set $(u_1^*, \ldots, u_4^*)$ which minimizes the objective function J in equation (11). That is,

$$J(u_1^*, \ldots, u_4^*) = \min_U J(u_1, \ldots, u_4), \tag{12}$$

where $U = \{(u_1, \ldots, u_4)$ such that $\{u_1, \ldots, u_4\}$ is a Lebeque measurable control set with $0 \le u_i(t) \le 1$, $i = 1, \ldots, 4$, for $t \in [0, t_f]\}$.

4.1. Existence of optimal solutions to the control problem

An optimal control solution is said to exist provided that the five necessary conditions that define the optimal solutions $J(u_1^*, \ldots, u_4^*) = \min_{(u_1,\ldots,u_4)\in U} J(u_1, \ldots, u_4)$ of system (1) are satisfied. The resulting optimality problem is solved based on Pontryagin's Maximum Principle (Anita et al., 2011).

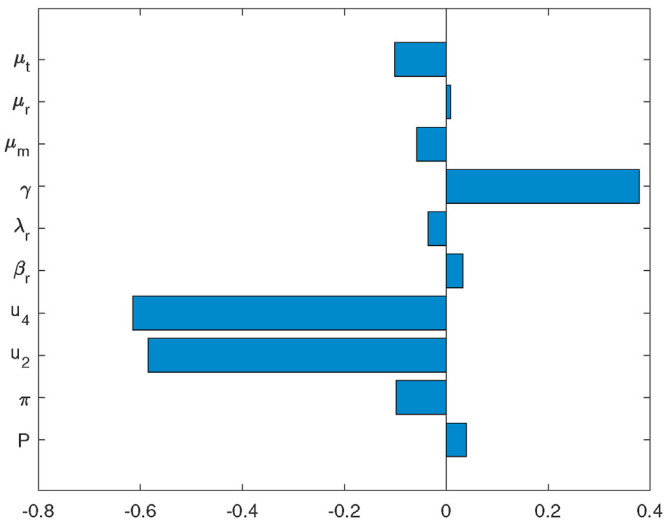

Fig. 1. Graph showing tornado plots of partial rank correlation coefficients (PRCCs) of the parameters that influence the effective reproduction number R_{eff}. Parameter values are shown in Table 2.

Theorem 4. *Consider an optimal problem* $\mathcal{N}(t, Y(t), u_i(t))$ *of system* (1)*, subject to initial conditions of state variable* $Y(t) \in \mathbb{R}^9_+$ *and boundary condition of control variables* $u_i(t) \in U$ *for* $i = 1, \ldots, 4$*. There exists an optimal solution* $J(u_1^*, \ldots, u_4^*)$ *such that* $J(u_1^*, \ldots, u_4^*) = \min_{(u_1,\ldots,u_4)\in U} J(u_1, \ldots, u_4)$ *if the following necessary conditions in* (Chuma, Mwanga, & Masanja, 2019) *are satisfied:*

(i) Control set U and the corresponding state variables are nonempty,
(ii) Control set U is convex and closed,
(iii) The right hand side of the state system is bounded by the linear function in the state and control variables,
(iv) The integrand of the objective function is convex, and
(v) There exist constant numbers $q_1, q_2 > 0$ and $\xi > 1$ such that the integrand of the objective function is bounded below by $q_1(|u_1| + |u_2| + |u_3| + |u_4|)^{\xi/2} - q_2$.

Proof: We verify the existence of an optimal control solution using the conditions provided by Fleming and Rishel (Fleming & Rishel, 1975). Given the optimal problem $\mathcal{N}(t, Y(t), u_i(t))$ of system (1), the set of state variables $Y(t) \in \mathbb{R}^9_+$ and the control variables $\{u_i(t) \in U | 0 \le u_i(t) \le 1\}$, $t \in [0, t_f]$ are non-negative. By definition, the optimal solution $u_i(t)$ is convex and bounded in U. Hence, the first (i) and second (ii) conditions is satisfied (Mlay, Luboobi, Kuznetsov, & Shahada, 2015; Mpeshe, Luboobi, & Nkansah-gyekye, 2014).

The differential system (1) is bounded. The third condition (iii) therefore holds. Moreover, the integrand in the objective functional in equation (11) is clearly convex on the control set U and the fourth condition also holds. Following the work by Lashara et al., (Lashari, Hattaf, Zaman, & Li, 2013), the integrand in equation (11) is also bounded below by

$$A_1X(t) + A_2T(t) + A_3M(t) + A_4G(t) + \frac{1}{2}\left(\sum_{i=1}^{4} B_i u_i^2\right) \ge q_1\left(\sum_{i=1}^{4} |u_i(t)|\right)^{\xi/2} - q_2 \tag{13}$$

for $i = 1, \ldots, 4$. This proves condition (v). The above five conditions are hence satisfied and

$$J(u_1^*, \ldots, u_4^*) = \min_U J(u_1, \ldots, u_4). \tag{14}$$

4.2. Characterisation of the optimal control

We employ Pontryagin's Maximum Principle (PMP) (Anita et al., 2011) in solving the stated optimal control problem. PMP converts the optimality system (1), objective function (11) and (12) into a problem of minimising a pointwise Hamiltonian H_a, with respect to controls $u_1 \cdots, u_4$. The Lagrangian L of the optimal control problem is given by

$$L = A_1X + A_2T + A_3M + A_4G + \frac{1}{2}(B_1u_1^2 + B_2u_2^2 + B_3u_3^2 + B_4u_4^2). \tag{15}$$

Clearly, the second derivatives of L in equation (15) with respect to u_i, $i = 1, \ldots, 4$, are all positive. This confirms that optimal control problem assumes a minimum value at the controls $u_1^*, \ldots, u_4^*$. We aim at obtaining the Lagrangian minimum value. This is accomplished by defining a Hamiltonian function H_a for the control problem. That is,

$$\begin{aligned} H_a &= L(X, T, M, G, u_1, u_2, u_3, u_4) + \Upsilon_1\dot{S} + \Upsilon_2\dot{H} + \Upsilon_3\dot{X} + \Upsilon_4\dot{R} + \Upsilon_5\dot{T} + \Upsilon_6\dot{C} + \Upsilon_7\dot{M} + \Upsilon_8\dot{G} + \Upsilon_9\dot{Z} \\ &= A_1X + A_2T + A_3M + A_4G + \frac{1}{2}(B_1u_1^2 + B_2u_2^2 + B_3u_3^2 + B_4u_4^2) + \Upsilon_1[\Lambda - \mu_sS - \beta_sSH] \end{aligned} \tag{16}$$

$$\begin{aligned} &+\Upsilon_2[\lambda_h - \mu_hH - (1-u_1(t))\beta_sSH] + \Upsilon_3\left[(1-u_1(t))\beta_sSH - \mu_xX - \frac{k_{xZX}}{1+\epsilon_0X}\right] + \Upsilon_4\left[\lambda_r - \frac{(1-u_2(t))\beta_rRM}{1+\alpha Z} - \mu_rR\right] \\ &+ \Upsilon_5\left[\frac{(1-u_2(t))\beta_{rRM}}{1+\alpha Z} - \mu_tT - \gamma T - \frac{k_{tZT}}{1+\epsilon_1T}\right] + \Upsilon_6\left[\gamma T - \mu_cC - \frac{k_cZC}{1+\epsilon_2C}\right] \\ &+ \Upsilon_7\left[(1-u_3(t))N\mu_xX + \frac{(1-u_4(t))P(1-\pi)\mu_cC}{1+\alpha Z} - \mu_mM - \beta_rRM\right] + \Upsilon_8\left[\pi\mu_cC - (u_3(t)+\mu_g)G\right] \\ &+ \Upsilon_9\left[\lambda_z + Z\left(\frac{\delta_xX}{1+\epsilon_0X} + \frac{\delta_tT}{1+\epsilon_1T} + \frac{\delta_cC}{1+\epsilon_2C}\right) - \mu_ZZ\right], \end{aligned} \tag{17}$$

where Υ_i, for $i = 1, \ldots, 9$, are the adjoint variables.

Theorem 5. *Let* $(S^*, H^*, X^*, R^*, T^*, C^*, M^*, G^*, Z^*)$ *and* $(u_1^*, \ldots, u_4^*)$ *be the solutions of the optimal control problem* (1) *and* (12) *and the solution of the optimal control measures, respectively. Then there exists adjoint variables* Υ_i, $i = 1, 2, \ldots, 9$ *satisfying*

$$
\left.
\begin{aligned}
\frac{d\Upsilon_1}{dt} &= (\Upsilon_2-\Upsilon_3)(1-u_1)\beta_s H+\Upsilon_1(\mu_s+\beta_s H),\\
\frac{d\Upsilon_2}{dt} &= (\Upsilon_1+(\Upsilon_2-\Upsilon_3)(1-u_1))\beta_s+\Upsilon_2\mu_h,\\
\frac{d\Upsilon_3}{dt} &= \frac{(\Upsilon_3 k_x-\Upsilon_9\delta_x)Z}{(1+\varepsilon_0 X)^2}-A_1+(\Upsilon_3-\Upsilon_7 N(1-u_3))\mu_x,\\
\frac{d\Upsilon_4}{dt} &= \frac{\beta_r((1+\alpha Z)\Upsilon_7+(1-u_2)(\Upsilon_4-\Upsilon_5))M}{(1+\alpha Z)}+\Upsilon_4\mu_r,\\
\frac{d\Upsilon_5}{dt} &= \frac{(\Upsilon_5 k_t-\Upsilon_9\delta_t)Z}{(1+\varepsilon_1 T)^2}+\Upsilon_5(\gamma+\mu_t)-(A_2+\gamma\Upsilon_6),\\
\frac{d\Upsilon_6}{dt} &= \Upsilon_6\left(\frac{k_c Z}{(1+\varepsilon_2 C)^2}+\mu_c\right)-\frac{\Upsilon_9\delta_c Z}{(1+\varepsilon_2 C)}-\pi\Upsilon_8\mu_c-\frac{(1-u_4)(1-\pi)P\Upsilon_7\mu_c}{(1+\alpha Z)},\\
\frac{d\Upsilon_7}{dt} &= \Upsilon_7(\beta_r R+\mu_m)-A_3+\frac{(\Upsilon_4-\Upsilon_5)(1-u_2)\beta_r R}{1+\alpha Z},\\
\frac{d\Upsilon_8}{dt} &= \Upsilon_8(u_3+\mu_g)-A_4,\\
\frac{d\Upsilon_9}{dt} &= \frac{\Upsilon_3 k_x X}{1+\varepsilon_0 X}+\frac{\Upsilon_6 k_c C}{1+\varepsilon_2 C}-\frac{\Upsilon_4(1-u_2)\alpha\beta_{rMR}}{(1+\alpha Z)^2}+\frac{\Upsilon_7(1-\pi)P(1-u_4)\alpha\mu_c C}{(1+\alpha Z)^2}\\
&\quad -\Upsilon_9\left(\frac{\delta_x X}{1+\varepsilon_0 X}+\frac{\delta_t T}{1+\varepsilon_1 T}+\frac{\delta_c C}{1+\varepsilon_2 C}-\mu_z\right)+\Upsilon_5\left(\frac{k_t T}{1+\varepsilon_1 T}+\frac{(1-u_2)\alpha\beta MR}{(1+\alpha Z)^2}\right),
\end{aligned}
\right\} \tag{18}
$$

with boundary conditions

$$\Upsilon_i(t_f)=0,\quad \text{for}\quad i=1,\ldots,9. \tag{19}$$

The optimal control measures are expressed as

$$u_i^*=\begin{cases}0 & \text{if } u_i\le 0,\\ u_i & \text{if } 0<u_i<1,\\ 1 & \text{if } u_i\ge 1.\end{cases} \tag{20}$$

Additionally, in the interior of the control set U, the optimal control measures $(u_1^*,\ldots,u_4^*)$ *are given by*

$$u_1^*=\max\left\{\min\left\{\frac{\beta_s(\Upsilon_3-\Upsilon_2)S^*H^*}{B_1},1\right\},0\right\} \tag{21}$$

$$u_2^*=\max\left\{\min\left\{\frac{\beta_r(\Upsilon_5-\Upsilon_4)R^*M^*}{(1+\alpha Z)B_2},1\right\},0\right\} \tag{22}$$

$$u_3^*=\max\left\{\min\left\{\frac{\Upsilon_8 G^*+\Upsilon_7\mu_x NX^*}{B_3},1\right\},0\right\} \tag{23}$$

$$u_4^*=\max\left\{\min\left\{\frac{\Upsilon_7\mu_c(1-\pi)PC^*}{(1+\alpha Z)B_4},1\right\},0\right\}. \tag{24}$$

Proof: See Appendix B.

4.3. Uniqueness of the optimality system

Having proved that both the state variables and the adjoint functions of the optimality system (1) and (12) are bounded and satisfy Lipschitz conditions (Caveny, 1970), the uniqueness of the optimal controls can easily be derived using the technique explained in (Kim et al., 2012).

Theorem 6. *The bounded solutions to the optimality system* (1) *and* (12) *are unique.*

Proof: See Appendix C.flushleft

The optimal controls are obtained through numerical simulations in the next section. The optimal control set $u_i^*, i = 1, \ldots, 4$ gives an optimal control strategy against in-host *P. falciparum* malaria infection.

5. Numerical simulations

Here, the backward-forward sweep (BFS) algorithm (Lenhart & Workman, 2007) and the 4th-order Runge-Kutta (RK) scheme in Matlab (Ince, 1943) are applied to solve the optimality system. The BFS algorithm has been implemented in several research studies (Joshi et al., 2006; Nakakawa, Mugisha, Shaw, Tinzaara, & Karamura, 2017; Namawejje, Luboobi, Kuznetsov, & Wobudeya, 2014; Okosun et al., 2011; Omondi et al., 2018). The optimal control code presented by Lenhart and Workman (Lenhart & Workman, 2007) was modified to generate numerical solutions to the optimality system (40)–(41). The state variables $\overline{x} = (S, H, X, R, T, C, M, G, Z)$ were solved forward in time using the 4th-order Runge-Kutta scheme in Matlab and the initial conditions (S_0, H_0, X_0, R_0, T_0, C_0, M_0, G_0, Z_0) and $\overline{u}_i$. The co-state system $\overline{\Upsilon}_i, i = 1, \ldots, 9$ was solved backward in time using the boundary conditions $\Upsilon_i(t_f) = 0$ and the values of $\overline{x}$ and $\overline{u}$. The control variables $\overline{u}$ were then updated in the second iteration by entering the new values of the state and co-state variables. This procedure is repeated till convergence is achieved.

The parameter values shown in Table 2 were obtained from literature. Other parameter values are however assumed. The retail price of ACTs in sub-Saharan Africa is roughly 5–7 US dollars ($) (Palafox et al., 2015). The median price of AL (the blood schizontocide) is $5.26, $6.03, $4.58, $5.36 and $5.36 in Uganda, Benin, Democratic Republic of the Congo, Nigeria and Zambia, respectively (Palafox et al., 2015). A study on the availability and retail prices of antimalarial drugs in rural Western Kenya revealed that the mean price of AL and DHA-PPQ was $4.5 and $4.39, respectively (Kioko et al., 2016). Penny et al.,(Penny et al., 2016), estimated the cost per dose of RTS,S/AS01 to be $6.52 ($2.69 –$12.9). In this study, and for purposes of this analysis, we shall assume an average retail price of $5 for AL and primaquine per dose. Additionally, the pre-erythrocytic vaccine (RTS,S/AS01) is considered highly cost-effective and is estimated to assume a cost of $5 per dose under a four-dose schedule (Winskill et al., 2017b). This implies a unit cost of $39.25 is incurred per fully vaccinated child (Penny et al., 2016; Winskill et al., 2017b). We further assume the blood-stage vaccine would bear a similar cost of $5 per dose. Therefore, the costs $A_1 = A_2 = \$39.25$. Similarly, $A_3 = A_4 = \$5$.

Malaria treatment using ACTs have made a significant contribution to current success in malaria control efforts. For the period 2014–2017, WHO spent about US $11.71, $13.70, $12.53 and $14.18 per malaria cases averted, respectively. The 2015 World malaria report showed that about 663 million malaria cases were averted for the period 2001–2015 (WHO, 2016); of these cases, 21% (17%, 29%) were averted due to ACT use. Therefore, an average of US $11.90 was spent per year on malaria cases averted by *ACTs* in the period 2014–2017. Additionally, a report by the President's Malaria Initiative (PMI), estimated that about US $94 (95% CI: $51, $166) was spent per disability adjusted life year (DALY) averted for the period 2005–2017 (Winskill et al., 2017a). This represents about US $7.80 per cases averted per year. Unlike the efficacies of antimalarial drugs (95%), the vaccines considered in this study have a moderate efficacy of 75%. The weight constants B_1, B_2, B_3 and B_4 are hence assigned a slightly lower average value of US $7.50. That is, $B_1 = B_2 = B_3 = B_4 = 7.50$.

Table 2
Table showing parameter values.

Parameter	Value	Range	Units	Source
P	16	(15–20)	Unitless	Diebner et al. (2000)
k_x, k_t, k_c	0.01	(0.001–0.9)	day^{-1}	Chiyaka et al. (2008)
μ_r	0.083	(0.05–0.1)	day^{-1}	Anderson, May, and Gupta (1989)
β_r	2.0×10^{-2}	(0.01–0.3)	$mm^{-3}day^{-1}$	Dondorp, Kager, Vreeken, and White (2000)
β_s	1.0×10^{-3}	(0.000 1–0.2)	$mm^{-3}day^{-1}$	Selemani, Luboobi, and Nkansah-Gyekye (2016)
π	0.2	(0.1–0.9)	unitless	Talman, Domarle, McKenzie, Ariey, and Robert (2004)
μ_h	0.029	(0.01–0.5)	day^{-1}	Estimated
μ_x	0.02	(0.01–1)	day^{-1}	Selemani et al. (2016)
λ_r	3×10^3	$(3 \times 10^2 - 3 \times 10^8)$	cells/ml day^{-1}	Li, Ruan, and Xiao (2011)
λ_h	3×10^4	$(3 \times 10^5 - 3 \times 10^8)$	cells $\mu l^{-1} day^{-1}$	Tumwiine, Mugisha, and Luboobi (2008)
λ_z	30	(10–40)	$\mu l^{-1} day^{-1}$	Chiyaka (2010)
μ_m	48	(46–50)	day^{-1}	Li et al. (2011)
Λ	30	(18–35)	sporozoites day^{-1}	Selemani et al. (2016)
μ_s	1.2	$(1.0 - 2.4)$	day^{-1}	Selemani et al. (2016)
μ_t	0.27	(0.01–0.8)	day^{-1}	Magombedze, Chiyaka, and Mukandavire (2011)
μ_c	0.7	(0.1–0.9)	day^{-1}	Magombedze et al. (2011)
μ_g	0.000 062 5	$(6.0 \times 10^{-5} - 7.0 \times 10^{-5})$	day^{-1}	Selemani et al. (2016)
μ_z	2	(0.5–3)	day^{-1}	Chiyaka (2010)
δ_x, δ_t, δ_c	1e-5	(1e-5-1e-7)	$mm^{-3}day^{-1}$	Chiyaka (2010)
γ	1.5	(0.1–2)	day^{-1}	Selemani et al. (2016)
ε_0, ε_1, ε_2	1E-5	(1E-6, 1E-4)	day^{-1}	Tumwiine et al. (2008)
α	0.000 5	(0.000 05–0.02)	unitless	Magombedze et al. (2011)
N	10 000	(8000–20 000)	Unitless	Tumwiine et al. (2008)

In this section, therefore, we assume that the coefficients $A_1 = A_2 = 39.25$, $A_3 = A_4 = 5.00$ and $B_i = 7.50$, $i = 1, \ldots, 4$. The initial conditions are also fixed at: $S(0) = 3000$, $H(0) = 3 \times 10^5$, $X(0) = 5 \times 10^2$, $R(0) = 5 \times 10^6$, $T(0) = 5 \times 10^3$, $C(0) = 5000$, $M(0) = 9000$, $G(0) = 5000$, $Z(0) = 3000$. The results of the effects of various control strategies against in-host *P. falciparum* malaria infections are as displayed in Figs. 2–13. We chose arbitrary initial conditions because the presented model (with *constant* vaccine controls) exhibits global stability behaviour. Note that we considered all the possible set of control combinations in this study. However, only those that gave substantial decrease in the populations (of X, T, M and G) as pre-defined in the objective functional (12) are presented. To simplify the analysis, the four control measures are grouped into the following six categories:

- Strategy 1: A combination of two control measures
  - (1A) A combination of blood schizontocide u_3 and gametocytocide u_4 only.
  - (1B) A combination of pre-erythrocytic u_1 and blood stage vaccine antigen u_2 only.
  - (1C) A combination of pre-erythrocytic vaccine u_1 and blood schizontocide drug u_3 only.
- Strategy 2: A combination of three control measures
  - (2A) Pre-erythrocytic vaccine antigen u_1, blood stage vaccine antigen u_2 and blood schizontocide u_3 only.
  - (2B) Pre-erythrocytic vaccine antigen u_1, blood schizontocide u_3 and gametocytocide u_4 only.
- Strategy 3: A combination of all the four control measures (pre-erythrocytic vaccine antigen u_1, blood stage vaccine antigen u_2, blood schizontocide u_3 and gametocytocide u_4).

5.1. Simulation results

The impact of employing strategy (1A) (a combination of blood schizontocide and gametocytocide only) in the control of *P. falciparum* malaria is presented in Fig. 2. It is evident that an antimalarial drug with such a combination is highly effective in eradicating the merozoites and infected erythrocytes as shown in Fig. 2b and c, respectively. However, this combination

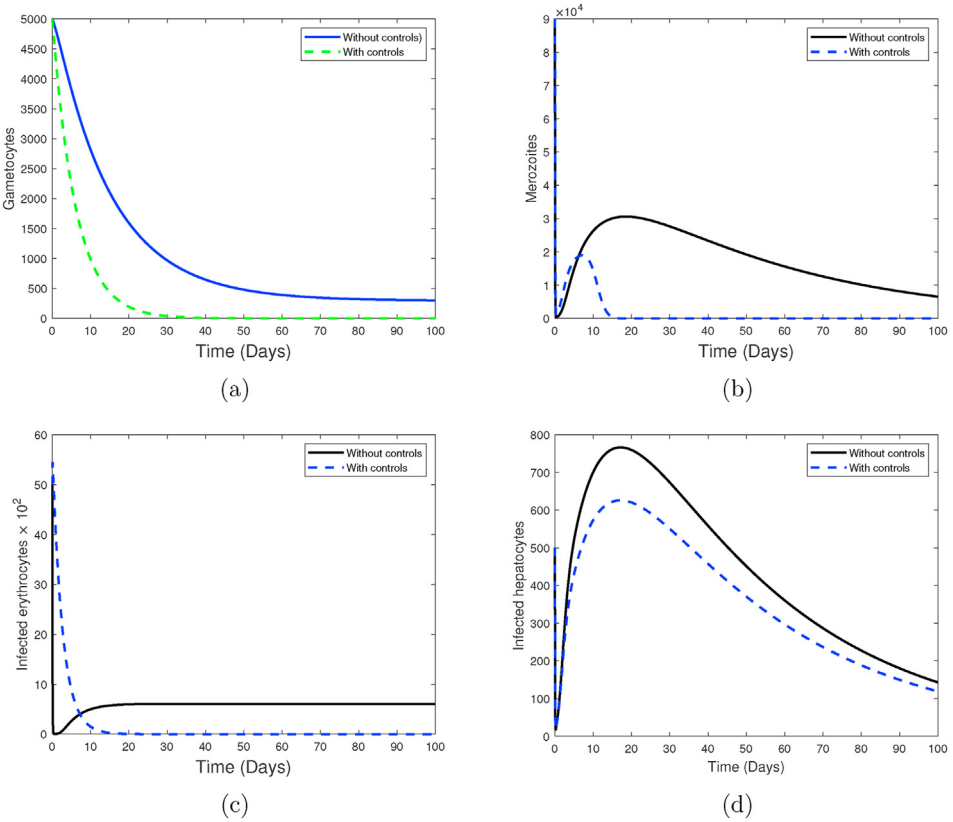

Fig. 2. Simulations of system (1), showing the impact of a combination of blood schizontocide u_3 and a gametocitocide u_4 only during clinical *P. falciparum* malaria infection. Used parameter values are shown in Table 2.

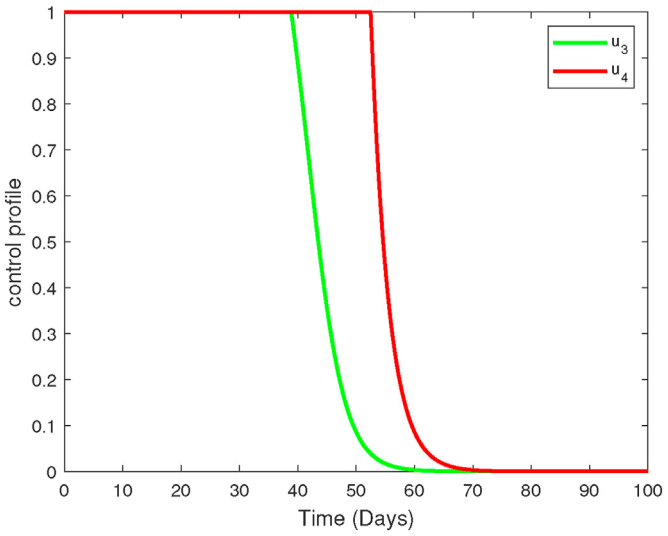

Fig. 3. Profiles of blood schizontocide u_3 and gametocytocide u_4. Here, $u_1 = 0$, $u_2 = 0$.

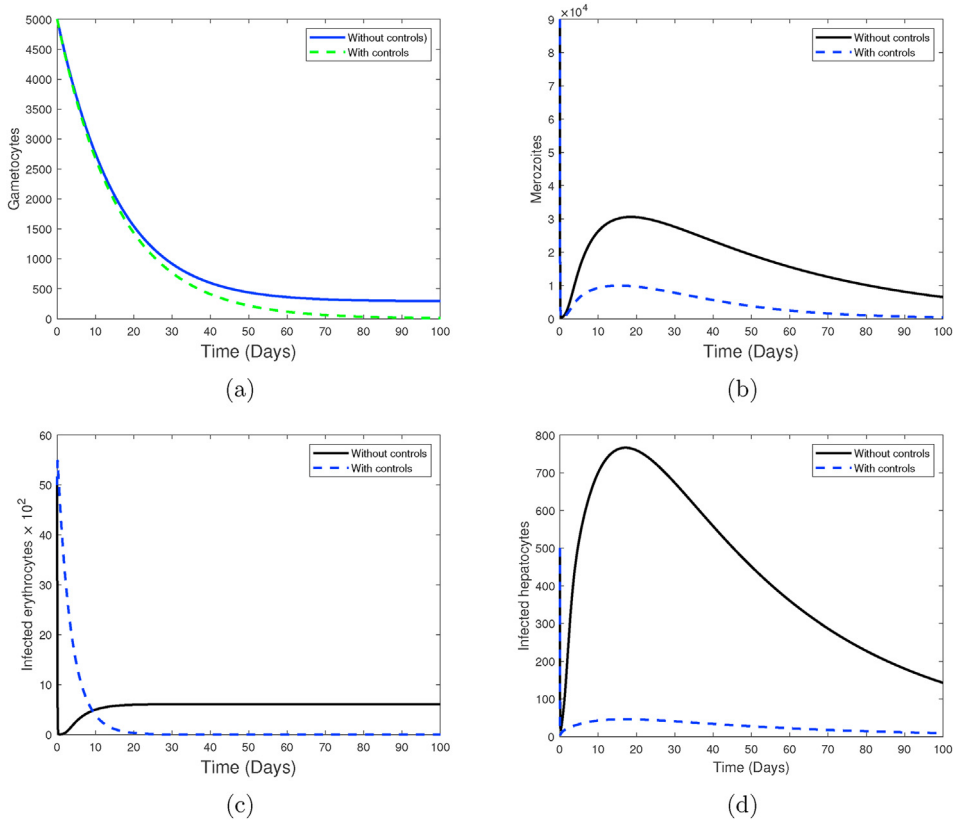

Fig. 4. Simulations of system (1), showing the impact of a combination of pre-erythrocytic vaccine antigens u_1 with blood stage vaccine antigens u_2 only. Used parameter values are shown in Table 2.

strategy offers little impact on the population of infected liver hepatocytes (see Fig. 2d). This is because these drugs are not active against the liver stage parasites or schizonts.

Moreover, a moderate decrease in the populations of gametocytes is also observed (see Fig. 2a). Besides effective anti-malarial drugs, it is clear that other therapeutic measures maybe necessary to eradicate all parasites and infected hepatocytes

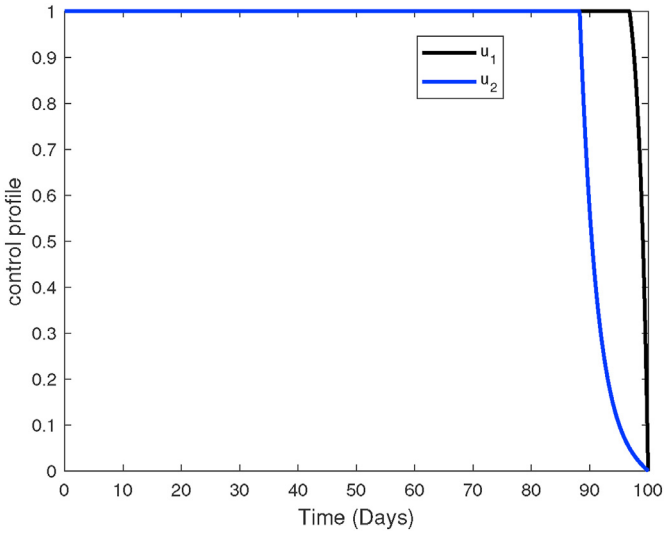

Fig. 5. Profiles of pre-erythrocytic vaccine antigen u_1 and blood stage vaccine antigens u_2. Here, $u_3 = 0$, $u_4 = 0$.

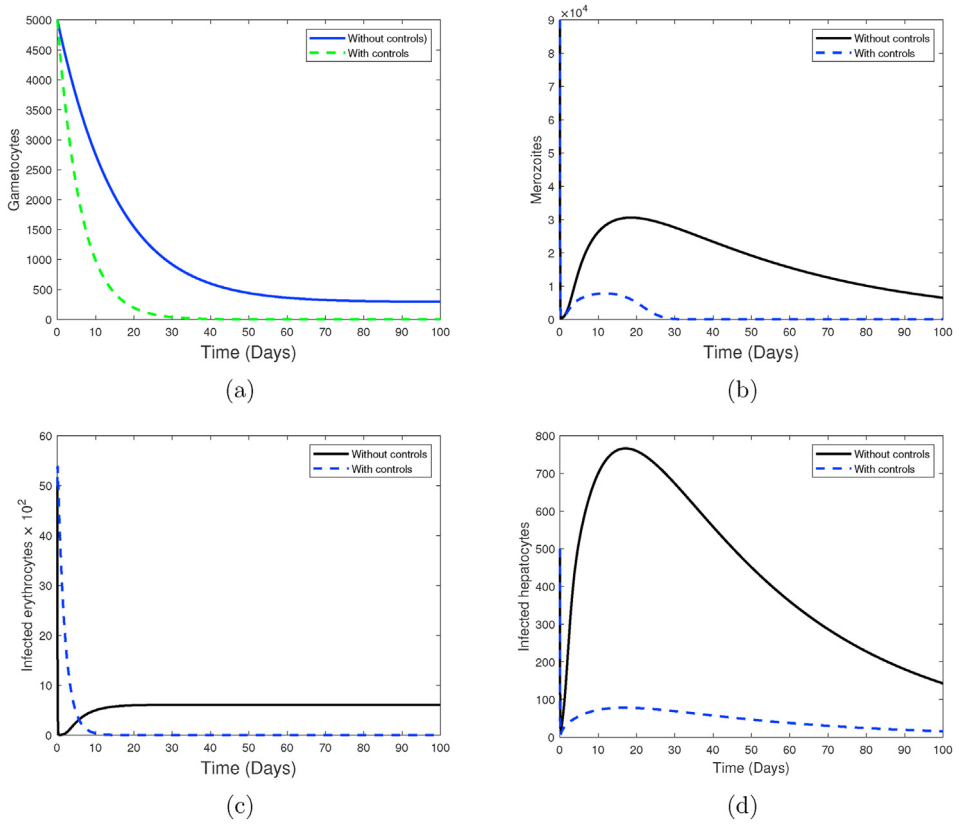

Fig. 6. Simulations of system (1), showing the impact of a combining pre-erythrocytic malaria vaccine u_1 and blood schizontocides u_3 only in the control of within-human *P. falciparum* infection. Used parameter values are shown in Table 2.

and erythrocytes during *P. falciparum* malaria infections. The control profile of strategy (1A) is shown in Fig. 3. Observe that the concentration of the blood schizontocide and gametocytocide should remain highest for the first three-quarter of the intervention period.

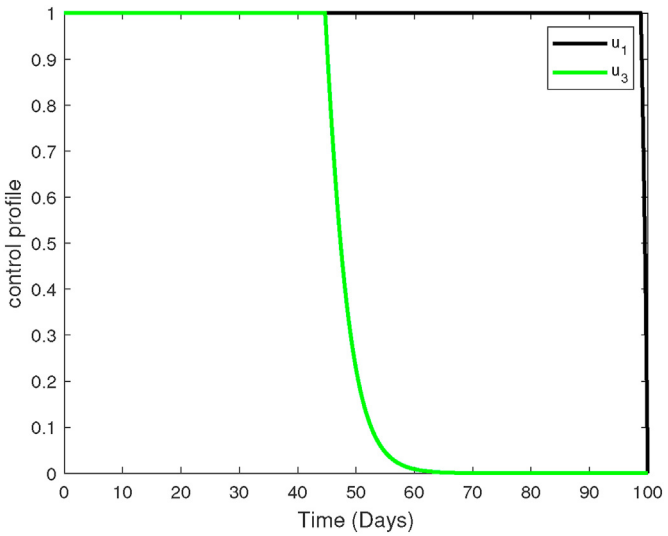

Fig. 7. Profiles of pre-erythrocytic vaccine antigen u_1 and blood schizontocide drug u_3. Here, $u_2 = 0$, $u_4 = 0$.

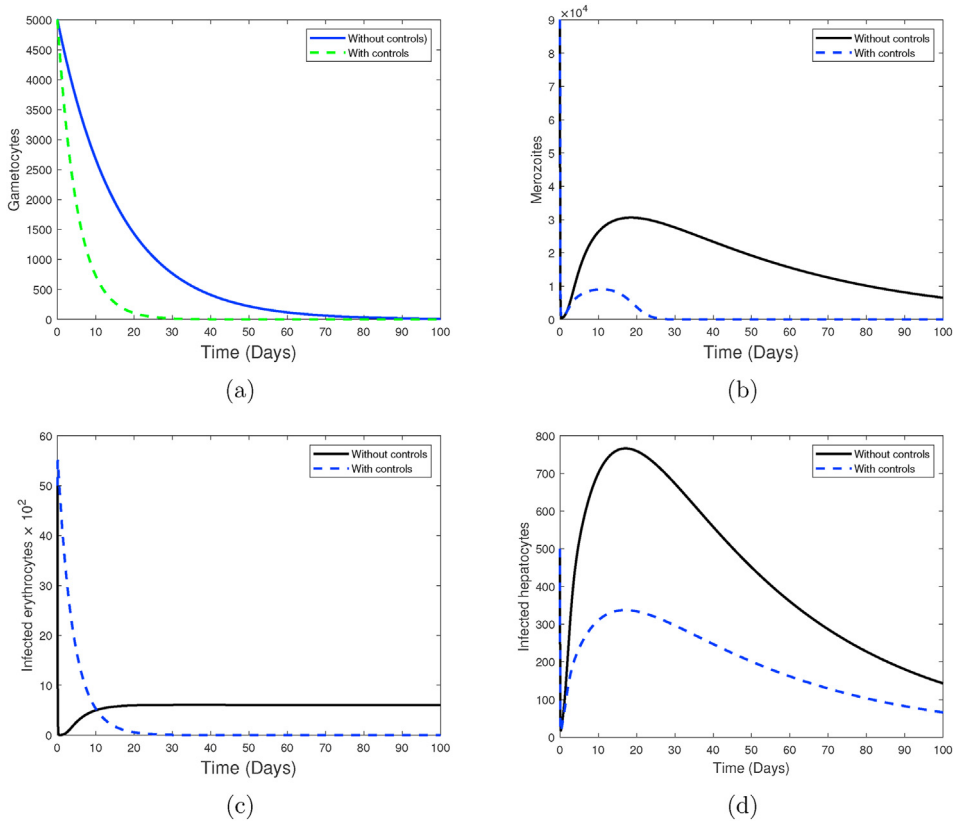

Fig. 8. Simulations of system (1), showing the impact of a combination of pre-erythrocytic vaccine antigens u_1, blood stage vaccine antigens u_2 and blood schizontocide u_3 only. Used parameter values are shown in Table 2.

In Fig. 4, a combination of malaria vaccine antigens is considered. This corresponds to strategy (1B). The combination of pre-erythrocytic vaccine antigen u_1 and blood-stage vaccine antigen u_2 is shown to be very effective in decreasing the populations of infected erythrocytes (Fig. 4c) and infected hepatocytes (Fig. 4d). Although the merozoites are eradicated, this takes a slightly longer time, due to low vaccine efficacies (see Fig. 4b). A 100% efficacy of PEV would, however, not require

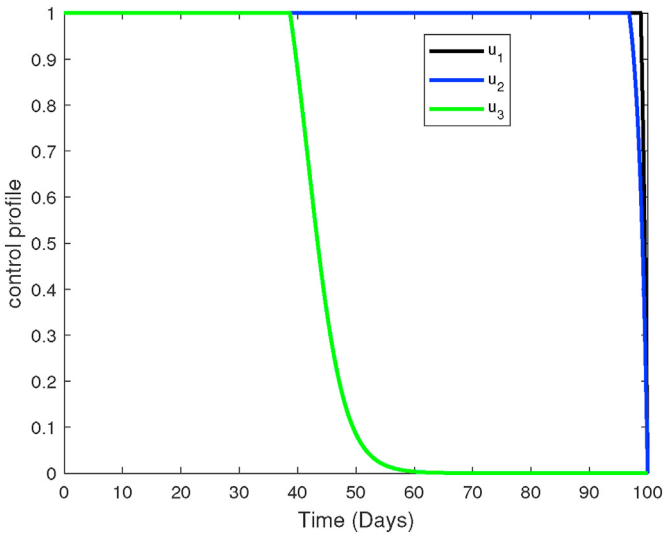

Fig. 9. Profiles of pre-erythrocytic vaccine antigen u_1, blood stage vaccine antigen u_2 and blood schizontocide u_3. Here, $u_4 = 0$.

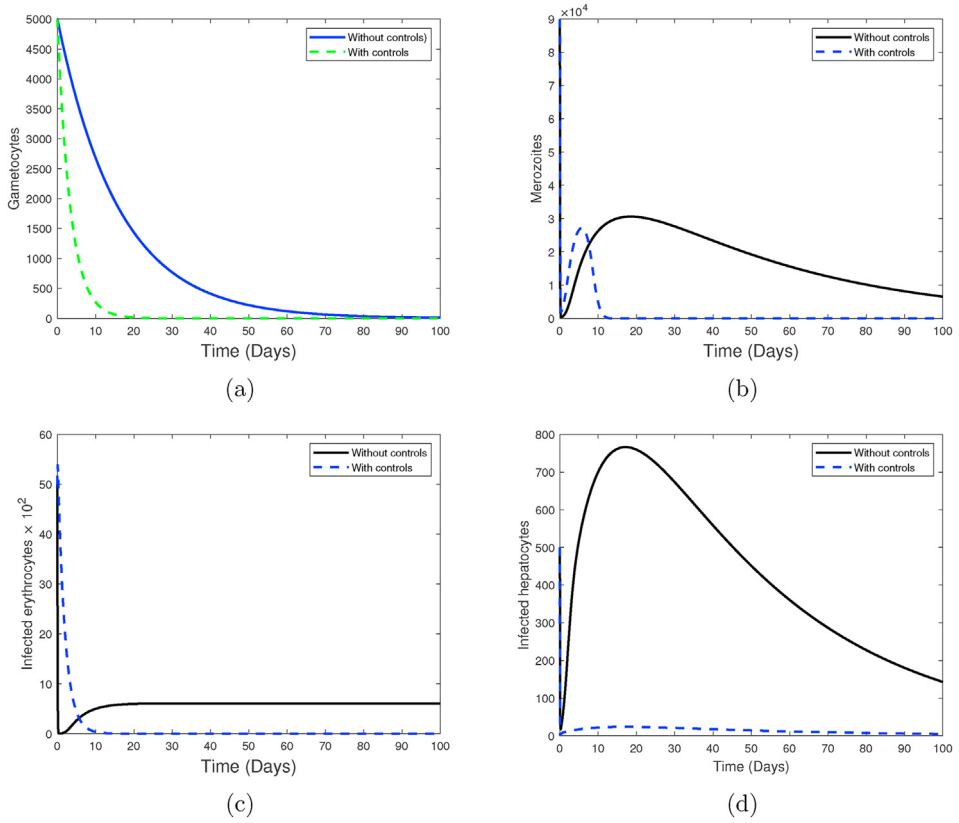

Fig. 10. Simulations of system (1), showing the impact of a combination of pre-erythrocytic malaria vaccine u_1, blood schizontocide u_3 and gametocitocidal drug u_4. Used parameter values are shown in Table 2.

augmenting with BSV. Nevertheless, the efficacies of PEV and BSV is still likely to drop over time as the antibodies decay (Sherrard-Smith et al., 2018). The control profile under this strategy is presented in Fig. 5. We observe that the efficacies of the vaccines should be maintained high for the entire period of intervention.

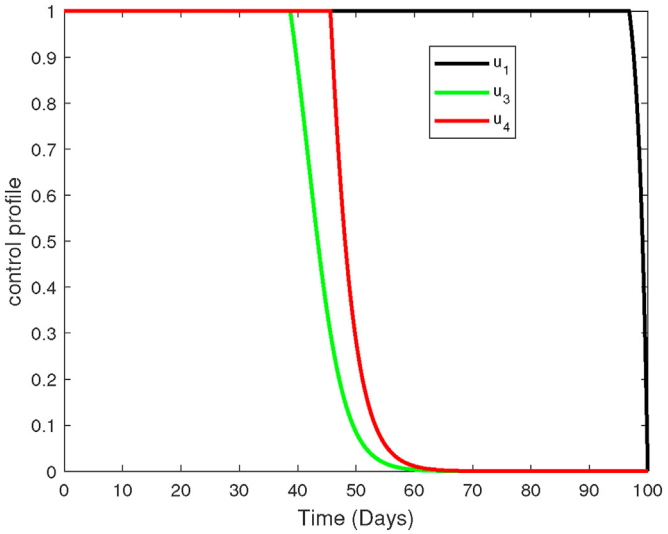

Fig. 11. Profiles of pre-erythrocytic vaccine antigen u_1, blood schizontocide u_3 and gametocytocide u_4. Here $u_2 = 0$.

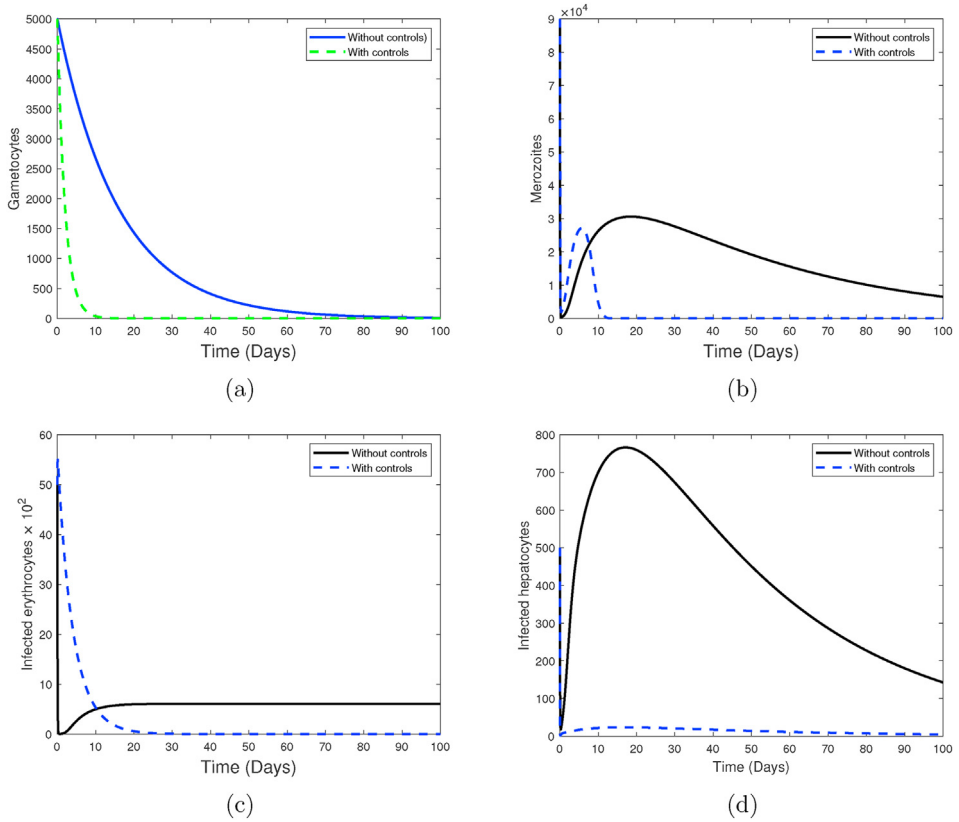

Fig. 12. Simulations of system (1), showing the impact of combining antigens of pre-erythrocytic malaria vaccine antigen u_1 and blood stage vaccine antigen u_2 together with the administration of combined blood schizontocide u_3 and gametocitocidal drug u_4. Used parameter values are shown in Table 2.

The combined use of pre-erythrocytic vaccine and blood schizontocide, strategy (1C), is shown to greatly decrease the population of infected erythrocytes and infected hepatocytes in Fig. 6c and d, respectively. Unlike strategies (1A) and (1B), this third strategy (IC) is slightly more effective; it eradicates the merozoites and gametocytes within 30 days of infection (see Fig. 6a and b). Additionally, this strategy has a maximum duration of 11 days before it eradicates all infected erythrocytes from

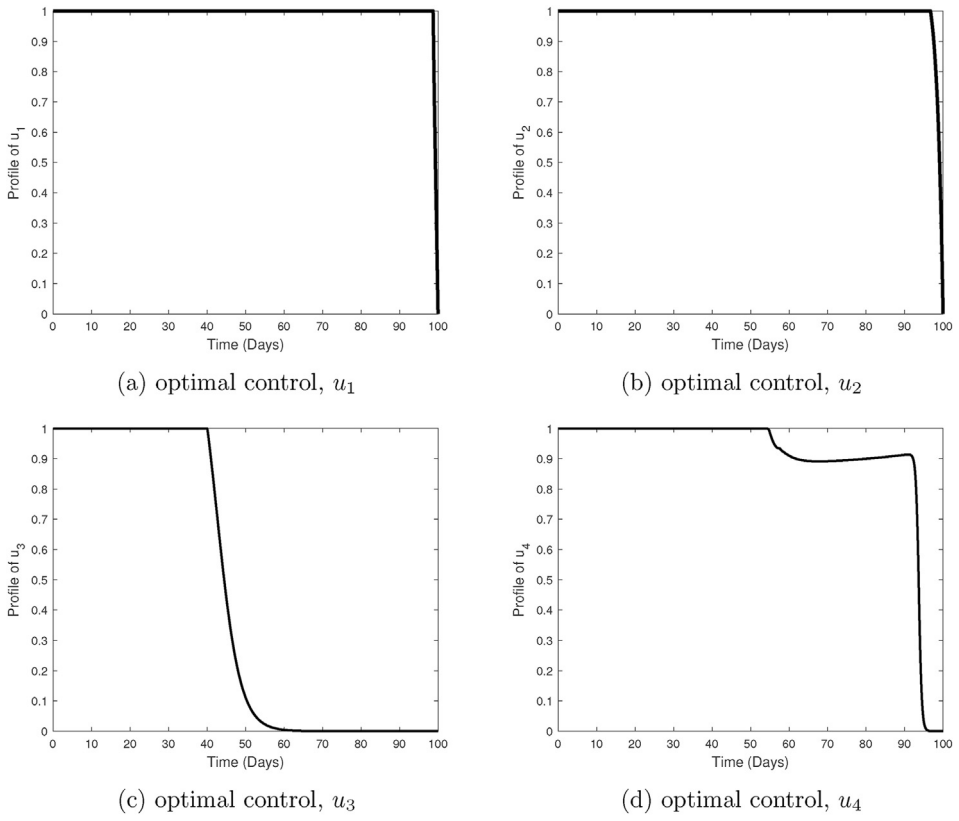

Fig. 13. Plots showing the control profiles of pre-erythrocytic vaccine antigen u_1, blood stage vaccine antigen u_2, blood schizontocide u_3 and gametocytocide u_4.

the host. To guarantee total eradication of all infected cells and infective parasites, the used antimalarial drug should be highly effective (efficacy $>$ 95%). The moderate effect of this strategy on the gametocyte population means that the treated malaria patients would facilitate parasite transmission to the mosquito vector, increasing future malaria cases and mortality. Fig. 7 shows the profile of the controls used in this strategy. The efficacy of the pre-erythrocyte vaccine (u_1) should be maintained throughout the control period. Similarly, the effectiveness of blood schizontocide (u_3) should remain high for at least half of the intervention period.

If we combine two or more vaccines and antimalarial drugs, then we observe different outcomes as presented in Figs. 8–13. In Fig. 8, blood schizontocide u_3 is used to treat malaria patients who have received a combination of pre-erythrocytic vaccine antigens u_1 and blood stage vaccine antigens u_2. This defines strategy (2A). The control profiles of $u_1 \neq 0$, $u_2 \neq 0$ and $u_3 \neq 0$ are presented in Fig. 9. A general decline in the populations of infected cells and infective parasite is observed in Fig. 8. However, the rate of decline is moderate and the clearance of gametocytes lasts longer than 20 days. A better result is however, presented in Fig. 10. In this strategy (2B), a combination of blood schizontocide u_3 and gametocytocides u_4 is administered to a malaria patient who is already on a pre-erythrocytic vaccine u_1. We observe a rapid rate of decline in populations of infected erythrocytes, infected hepatocytes, merozoites and gametocytes. The density of gametocytes fall exponentially; within 15 days of blood stage malaria. We also observe total eradication of the merozoite parasites from the human host within two weeks of infection. The profiles of the three controls are as displayed in Fig. 11.

Finally, in Fig. 12, all the four control efforts are employed (strategy 3). Here, antimalarial drugs consisting of blood schizontocides and gametocytocides are administered to malaria patients who are on pre-erythrocytic and blood stage vaccine antigens. Just like in strategy (2B), we observe tremendous decline in the populations of gametocytes, merozoites, infected hepatocytes and infected erythrocytes when all the controls are employed. It takes a much shorter time to eliminate malaria merozoites. Both the merozoites and infected red blood cells get eradicated within 12 days of infection. It is clear that both strategy (2B) and strategy 3 offer the best control options against *P. falciparum* malaria infection. Moreover, the simulations results in Figs. 10 and 12 reveal that the emergence of clinical malaria would be least likely if either of these control strategies is implemented correctly. Nevertheless, strategy (2B) only needs one highly efficacious malaria vaccine to achieve the same result as that in strategy 3. Additionally, strategy (2B) is likely to be less costly compared to strategy 3, which incorporates all the four controls. We therefore conclude that the optimal control strategy against *P. falciparum* malaria is strategy (2B): a combination of efficacious pre-erythrocytic vaccine, effective blood schizontocide and a gametocytocide.

The profiles of the four controls employed in strategy 3 are shown in Fig. 13. It is observed that the control profiles of the pre-erythrocytic vaccine (u_1) and blood stage vaccines antigens (u_2) are maintained at highest levels of efficacy (75% in our case) to ensure maximum eradication of asexual sporozoites and infected erythrocytes, respectively. Similarly, the concentrations of blood schizontocides (u_3) and gametocytocides (u_4) should be maintained at the highest levels ($\geq$ 95% in our case) to maximize eradication of asexual merozoites and infected erythrocytes, respectively. Like in other control strategies already discussed, the effectiveness of the antimalarial drugs is likely to fall after day 45 and this remains lowest till the end of the intervention period.

The best control strategy of an in-host malaria infection should eradicate all infective merozoites, infected hepatocytes and infected red blood cells within the shortest time possible at a minimal cost. Epidemiologically, the best control strategy should ensure no gametocyte parasites are available for transmission to the mosquito vector. Although strategy (2B) is the optimal in-host malaria control strategy (according to our study), it should be implemented alongside existing vector control measures such as ITNs and IRS if malaria elimination goal is to be achieved (WHO, 2015a). This result is crucial for malaria drug development and highlights the urgent need for a highly efficacious pre-erythrocytic malaria vaccine to complement existing ACTs.

6. Conclusion

In this study, the theory of optimal control has been applied to an in-host malaria model. The model incorporates antimalarial drugs and malaria vaccines as control strategies against *P. falciparum* malaria. The objective was to establish the best combination strategy involving (1) a blood schizontocide (2) a gametocytocide (3), a pre-erythrocytic vaccine antigen and (4) blood stage vaccine antigen against *P. falciparum* malaria. The Pontryagin's Maximum Principle was used to characterize the control strategies that substantially reduced the populations of infected erythrocytes, infected hepatocytes and malaria parasites. The necessary conditions for the existence of the optimal control solutions were derived and mathematically analyzed. For sufficiently small values of intervention time, we proved the uniqueness of the optimality system.

Numerical results showed that a combination of pre-erythrocytic vaccine, blood schizontocide and gametocytocide drugs would offer the best control strategy against clinical *P. falciparum* malaria. A combination of all the four controls equally gave a comparatively good results, however, it may be too expensive. Nonetheless, the synergy of malaria vaccine antigens and antimalarial drug regimens is crucial for future malaria chemotherapy control. Moreover, sensitivity analysis revealed that in-host malaria infection dynamics is heavily influenced by the efficacy antimalarial drugs that target blood trophozoites and blood schizonts. To limit or minimize the severity of clinical malaria infections, an effective anti-malarial drug should be used alongside efficacious blood stage vaccine.

Note that the parameter values and weights used in this study are estimated for illustration purposes. Availability of data on the costs of implementation of the four controls is likely to present a much better model outcome. However, the results presented in this paper gives insights on the need to combine effective antimalarial drugs and to use them alongside efficacious malaria vaccine antigens to control *P. falciparum* malaria infections within the human host. In light of these results, cost effectiveness analysis of the presented controls would form part of our future investigation.

Funding

The authors received no direct funding for this research.

Availability of data and materials

All data used in this study are included in this published article.

Authors' contributions

All authors contributed to all sections of this manuscript.

Ethical approval and consent to participate

Not applicable.

Consent for publication

Not applicable.

Declaration of competing interest

The authors declare that there is no conflict of interest regarding the publication of this article.

Acknowledgement

The authors acknowledge the support of the Strathmore Institute of Mathematical Sciences is in Nairobi, Kenya in the production of this manuscript. They are also very grateful to the anonymous reviewers for their careful reading and constructive comments.

Appendix AProof of Theorem 3

Based on the property of $\mathcal{E}_d$ (Kamgang & Sallet, 2005), it is possible to rewrite system (1) in pseudo-triangular form as follows:

$$\begin{aligned}\dot{X}_1 &= B_1(X_1 - X_1^*) + B_2X_2,\\ \dot{X}_2 &= B_3X_2,\end{aligned}$$

where X_1 is the vector representing the non-transmitting states (susceptible hepatocytes H, susceptible erythrocytes R and $CD8^+$ T cells Z). The populations in these compartments are not infected with malaria parasites and do not therefore transmit malaria infections. So $X_1 = (H,R,Z)^t$. The vector X_2 represents the compartments that are responsible for disease transmission. These states are infected and or infective. Therefore $X_2 = (S,X,T,C,M,G)^t$, $X = (X_1, X_2)$ and $X_1^* = \left(\frac{\lambda_h}{\mu_h}, \frac{\lambda_r}{\mu_r}, \frac{\lambda_z}{\mu_z}\right)$.

Using the conditions at $\mathcal{E}_d$, subsystem X_1 gives

$$B_1(X) = \begin{pmatrix} -\mu_h & 0 & 0\\ 0 & -\mu_r & 0\\ 0 & 0 & -\mu_z \end{pmatrix}; \quad B_2(X) = \begin{pmatrix} \frac{-(1-u_1)\beta_s\lambda_h}{\mu_h} & 0 & 0 & 0 & 0 & 0\\ 0 & 0 & 0 & 0 & \frac{-(1-u_2)\beta_r\lambda_r\mu_z}{\mu_r(\alpha\lambda_z+\mu_z)} & 0\\ 0 & \frac{\delta_x\lambda_z}{\mu_z} & \frac{\delta_t\lambda_z}{\mu_z} & \frac{\delta_c\lambda_z}{\mu_z} & 0 & 0 \end{pmatrix}. \tag{25}$$

Clearly, the eigenvalues of matrix $B_1(X)$ in (25) are real and negative, showing that system $\dot{X}_1 = B_1(X)(X_1 - X_1^*) + B_2(X)X_2$ is globally asymptotically stable at $\mathcal{E}_d$. Moreover, subsystem X_2 gives matrix $B_3(X)$:

$$B_3(X) = \begin{pmatrix} \frac{-\beta_s\lambda_h}{\mu_h} - \mu_s & 0 & 0 & 0 & 0 & 0\\ \frac{(1-u_1)\beta_s\lambda_h}{\mu_h} & -\mu_x - \frac{k_x\lambda_z}{\mu_z} & 0 & 0 & 0 & 0\\ 0 & 0 & -\gamma - \mu_t - \frac{k_t\lambda_z}{\mu_z} & 0 & -\frac{(1-u_2)\beta_r\lambda_r\mu_z}{\mu_r(\alpha\lambda_z+\mu_z)} & 0\\ 0 & 0 & \gamma & -\mu_c - \frac{k_c\lambda_z}{\mu_z} & 0 & 0\\ 0 & 0 & 0 & \frac{P(1-\pi)(1-u_4)\mu_c\mu_z}{\alpha\lambda_z+\mu_z} & -\mu_m - \frac{\beta_r\lambda_r}{\mu_r} & 0\\ 0 & 0 & 0 & \pi\mu_c & 0 & -u_3 - \mu_g \end{pmatrix}. \tag{26}$$

Observe that $B_3(X)$ is a Metzler matrix. The equilibrium point $\mathcal{E}_d$ is globally asymptotically stable if the matrix $B_3(X)$ is Metzler stable. The stability of $B_3(X)$ is based on the following result:

Lemma 1. *Let M be a square Metzler matrix which is block decomposed:*

$$M = \begin{pmatrix} M_{11} & M_{12}\\ M_{21} & M_{22} \end{pmatrix},$$

where M_{11} and M_{22} are square matrices. The matrix M is Metzler stable if and only if M_{11} and $M_{22} - M_{21}M_{11}^{-1}M_{12}$ are Metzler stable.

In this analysis, the matrix M is simply matrix B_3 in (26). We therefore have flushleft

$$M_{11} = \begin{pmatrix} \frac{-\beta_s\lambda_h}{\mu_h} - \mu_s & 0 & 0 \\ \frac{(1-u_1)\beta_s\lambda_h}{\mu_h} & -\mu_x - \frac{k_x\lambda_z}{\mu_z} & 0 \\ 0 & 0 & -\gamma - \mu_t - \frac{k_t\lambda_z}{\mu_z} \end{pmatrix}, \quad M_{12} = \begin{pmatrix} 0 & 0 & 0 \\ 0 & 0 & 0 \\ 0 & -\frac{(1-u_2)\beta_r\lambda_r\mu_z}{\mu_r(\alpha\lambda_z+\mu_z)} & 0 \end{pmatrix},$$

$$M_{21} = \begin{pmatrix} 0 & 0 & \gamma \\ 0 & 0 & 0 \\ 0 & 0 & 0 \end{pmatrix} \text{ and } M_{22} = \begin{pmatrix} -\mu_c - \frac{k_c\lambda_z}{\mu_z} & 0 & 0 \\ \frac{P(1-\pi)(1-u_4)\mu_c\mu_z}{\alpha\lambda_z+\mu_z} & -\mu_m - \frac{\beta_r\lambda_r}{\mu_r} & 0 \\ \pi\mu_c & 0 & -u_3 - \mu_g \end{pmatrix}. \tag{27}$$

Upon computation in Mathematica software, we obtain

$$M_{22} - M_{21}M_{11}^{-1}M_{12} = \begin{pmatrix} -\mu_c - \frac{k_c\lambda_z}{\mu_z} & 0 & 0 \\ \frac{P(1-\pi)(1-u_4)\mu_c\mu_z}{\alpha\lambda_z+\mu_z} & -\mu_m - \frac{\beta_r\lambda_r}{\mu_r} & 0 \\ \pi\mu_c & 0 & -u_3 - \mu_g \end{pmatrix}. \tag{28}$$

Clearly, matrix $M_{22} - M_{21}M_{11}^{-1}M_{12}$ in (28) is Metzler stable matrix whenever $R_{eff} < 1$. Results in Lemma (1) yields Theorem 3.

Appendix B. Proof of Theorem 5

The presented adjoint system and the boundary conditions therein are standard results from the PMP (Anita et al., 2011). To obtain the differential equations governing the adjoint or co-state variables, we first set $S = S^*$, $H = H^*$, $X = X^*$, $R = R^*$, $T = T^*$, $C = C^*$, $M = M^*$, $G = G^*$ and $Z = Z^*$, and differentiate (partially) the Hamiltonian function H_a in equation (17) with respect to each of the state variables (S, H, X, R, T, C, M, G and Z). Thus,

$$\frac{d\Upsilon_1}{dt} = -\frac{\partial H_a}{\partial X}; \quad \Upsilon_1(t_f) = 0, \tag{29}$$

$$\frac{d\Upsilon_2}{dt} = -\frac{\partial H_a}{\partial H}; \quad \Upsilon_2(t_f) = 0, \tag{30}$$

$$\vdots$$

$$\frac{d\Upsilon_9}{dt} = -\frac{\partial H_a}{\partial Z}; \quad \Upsilon_9(t_f) = 0. \tag{31}$$

To obtain the optimality equations (21)-(24), we first differentiate partially the Hamiltonian function H_a with respect to the controls (u_1, …, u_4) and then solve for u_i^* (optimal control) by equating the derivatives to zero. Thus,

$$\frac{\partial H_a}{\partial u_1}|_{u_1^*} = \beta_s(\Upsilon_2 - \Upsilon_3)S^*H^* + B_1u_1^* = 0. \tag{32}$$

Making u_1^* the subject of the formula in equation (32), we obtain

$$u_1^*(t) = \frac{\beta_s(\Upsilon_3 - \Upsilon_2)S^*H^*}{B_1}. \tag{33}$$

Application of the above procedure to the rest of the controls yields:

$$u_2^* = \frac{\beta_r(\Upsilon_5 - \Upsilon_4)R^*M^*}{(1+\alpha Z)B_2}, \quad u_3^* = \frac{\Upsilon_8 G^* + \Upsilon_7 \mu_x N X^*}{B_3}, \quad u_4^* = \frac{\Upsilon_7 \mu_c (1-\pi) P C^*}{(1+\alpha Z)B_4}. \tag{34}$$

$$u_1^* = \begin{cases} 0 & \text{if} \quad \dfrac{\beta_s(\Upsilon_3 - \Upsilon_2)S^*H^*}{B_1} \le 0, \\ \dfrac{\beta_s(\Upsilon_3 - \Upsilon_2)S^*H^*}{B_1} & \text{if} \quad 0 < u_1 < 1, \\ 1 & \text{if} \quad \dfrac{\beta_s(\Upsilon_3 - \Upsilon_2)S^*H^*}{B_1} \ge 1. \end{cases} \tag{35}$$

The solution u_1^* is therefore expressed as

$$u_1^* = \max\left\{ \min\left\{ \frac{\beta_s(\Upsilon_3 - \Upsilon_2)S^*H^*}{B_1}, 1 \right\}, 0 \right\}. \tag{36}$$

Similarly, the optimal solutions u_2^*, u_3^* and u_4^* are expressed as follows:

$$u_2^* = \max\left\{ \min\left\{ \frac{\beta_r(\Upsilon_5 - \Upsilon_4)R^*M^*}{(1+\alpha Z)B_2}, 1 \right\}, 0 \right\} \tag{37}$$

$$u_3^* = \max\left\{ \min\left\{ \frac{\Upsilon_8 G^* + \Upsilon_7 \mu_x N X^*}{B_3}, 1 \right\}, 0 \right\} \tag{38}$$

$$u_4^* = \max\left\{ \min\left\{ \frac{\Upsilon_7 \mu_c (1-\pi) P C^*}{(1+\alpha Z)B_4}, 1 \right\}, 0 \right\}. \tag{39}$$

Utilizing the characteristic functions in equations (21)-(24), the following optimality system (40)–(41) characterizes the optimal control:

$$\left.\begin{aligned}
\frac{dS}{dt} &= \Lambda - \mu_s S - \beta_s S H, \\
\frac{dH}{dt} &= \lambda_h - \mu_h H - \left(1 - \max\left\{ \min\left\{ \frac{\beta_s(\Upsilon_3 - \Upsilon_2)S^*H^*}{B_1}, 1 \right\}, 0 \right\} \right)\beta_s S H, \\
\frac{dX}{dt} &= \left(1 - \max\left\{ \min\left\{ \frac{\beta_s(\Upsilon_3 - \Upsilon_2)S^*H^*}{B_1}, 1 \right\}, 0 \right\} \right)\beta_s S H - \mu_x X - \frac{k_{xZX}}{1+\epsilon_0 X}, \\
\frac{dR}{dt} &= \lambda_r - \frac{\left(1 - \max\left\{ \min\left\{ \frac{\beta_r(\Upsilon_5 - \Upsilon_4)R^*M^*}{(1+\alpha Z)B_2}, 1 \right\}, 0 \right\} \right)\beta_r R M}{1+\alpha Z} - \mu_r R, \\
\frac{dT}{dt} &= \frac{\left(1 - \max\left\{ \min\left\{ \frac{\beta_r(\Upsilon_5 - \Upsilon_4)R^*M^*}{(1+\alpha Z)B_2}, 1 \right\}, 0 \right\} \right)\beta_{rRM}}{1+\alpha Z} - \mu_t T - \gamma T - \frac{k_{tZT}}{1+\epsilon_1 T}, \\
\frac{dC}{dt} &= \gamma T - \mu_c C - \frac{k_c Z C}{1+\epsilon_2 C}, \\
\frac{dM}{dt} &= \left(1 - \max\left\{ \min\left\{ \frac{\Upsilon_8 G^* + \Upsilon_7 \mu_x N X^*}{B_3}, 1 \right\}, 0 \right\} \right) N \mu_x X \\
&\quad + \frac{\left(1 - \max\left\{ \min\left\{ \frac{\Upsilon_7 \mu_c (1-\pi) P C^*}{(1+\alpha Z)B_4}, 1 \right\}, 0 \right\} \right) P(1-\pi)\mu_c C}{1+\alpha Z} - \mu_m M - \beta_r R M, \\
\frac{dG}{dt} &= \pi \mu_c C - \left(\left(\max\left\{ \min\left\{ \frac{\Upsilon_8 G^* + \Upsilon_7 \mu_x N X^*}{B_3}, 1 \right\}, 0 \right\} \right) + \mu_g \right) G,
\end{aligned}\right\} \tag{40}$$

$$
\left.
\begin{aligned}
\frac{dZ}{dt} &= \lambda_z + Z\left(\frac{\delta_x X}{1+\epsilon_0 X} + \frac{\delta_t T}{1+\epsilon_1 T} + \frac{\delta_c C}{1+\epsilon_2 C}\right) - \mu_Z Z,\\
\frac{d\Upsilon_1}{dt} &= (\Upsilon_2 - \Upsilon_3)\left(1 - \max\left\{\min\left\{\frac{\beta_s(\Upsilon_3 - \Upsilon_2)S^* H^*}{B_1}, 1\right\}, 0\right\}\right)\beta_s H + \Upsilon_1(\mu_s + \beta_s H),\\
\frac{d\Upsilon_2}{dt} &= \left(\Upsilon_1 + (\Upsilon_2 - \Upsilon_3)\left(1 - \max\left\{\min\left\{\frac{\beta_s(\Upsilon_3 - \Upsilon_2)S^* H^*}{B_1}, 1\right\}, 0\right\}\right)\right)\beta_s + \Upsilon_2\mu_h,\\
\frac{d\Upsilon_3}{dt} &= \frac{(\Upsilon_3 k_x - \Upsilon_9\delta_x)Z}{(1+\varepsilon_0 X)^2} - A_1 + \left(\Upsilon_3 - \Upsilon_7 N\left(1 - \max\left\{\min\left\{\frac{\Upsilon_8 G^* + \Upsilon_7\mu_x N X^*}{B_3}, 1\right\}, 0\right\}\right)\right)\mu_x,\\
\frac{d\Upsilon_4}{dt} &= \frac{\beta_r\left((1+\alpha Z)\Upsilon_7 + \left(1 - \max\left\{\min\left\{\frac{\beta_r(\Upsilon_5 - \Upsilon_4)R^* M^*}{(1+\alpha Z)B_2}, 1\right\}, 0\right\}\right)(\Upsilon_4 - \Upsilon_5)\right)M}{(1+\alpha Z)} + \Upsilon_4\mu_r,\\
\frac{d\Upsilon_5}{dt} &= \frac{(\Upsilon_5 k_t - \Upsilon_9\delta_t)Z}{(1+\varepsilon_1 T)^2} + \Upsilon_5(\gamma + \mu_t) - (A_2 + \gamma\Upsilon_6),\\
\frac{d\Upsilon_6}{dt} &= \Upsilon_6\left(\frac{k_c Z}{(1+\varepsilon_2 C)^2} + \mu_c\right) - \frac{\left(1 - \max\left\{\min\left\{\frac{\Upsilon_7\mu_c(1-\pi)PC^*}{(1+\alpha Z)B_4}, 1\right\}, 0\right\}\right)(1-\pi)P\Upsilon_7\mu_c}{(1+\alpha Z)}\\
&\quad - \frac{\Upsilon_9\delta_c Z}{(1+\varepsilon_2 C)} - \pi\Upsilon_8\mu_c,\\
\frac{d\Upsilon_7}{dt} &= \Upsilon_7(\beta_r R + \mu_m) - A_3 + \frac{(\Upsilon_4 - \Upsilon_5)\left(1 - \max\left\{\min\left\{\frac{\beta_r(\Upsilon_5 - \Upsilon_4)R^* M^*}{(1+\alpha Z)B_2}, 1\right\}, 0\right\}\right)\beta_r R}{1+\alpha Z},\\
\frac{d\Upsilon_8}{dt} &= \Upsilon_8\left(\left(\max\left\{\min\left\{\frac{\Upsilon_8 G^* + \Upsilon_7\mu_x N X^*}{B_3}, 1\right\}, 0\right\}\right) + \mu_g\right) - A_4,\\
\frac{d\Upsilon_9}{dt} &= \frac{\Upsilon_3 k_x X}{1+\varepsilon_0 X} + \frac{\Upsilon_6 k_c C}{1+\varepsilon_2 C} - \frac{\Upsilon_4\left(1 - \max\left\{\min\left\{\frac{\beta_r(\Upsilon_5 - \Upsilon_4)R^* M^*}{(1+\alpha Z)B_2}, 1\right\}, 0\right\}\right)\alpha\beta_{rMR}}{(1+\alpha Z)^2}\\
&\quad + \frac{\Upsilon_7(1-\pi)P\left(1 - \max\left\{\min\left\{\frac{\Upsilon_7\mu_c(1-\pi)PC^*}{(1+\alpha Z)B_4}, 1\right\}, 0\right\}\right)\alpha\mu_c C}{(1+\alpha Z)^2}\\
&\quad - \Upsilon_9\left(\frac{\delta_x X}{1+\varepsilon_0 X} + \frac{\delta_t T}{1+\varepsilon_1 T} + \frac{\delta_c C}{1+\varepsilon_2 C} - \mu_z\right)\\
&\quad + \Upsilon_5\left(\frac{k_t T}{1+\varepsilon_1 T} + \frac{\left(1 - \max\left\{\min\left\{\frac{\beta_r(\Upsilon_5 - \Upsilon_4)R^* M^*}{(1+\alpha Z)B_2}, 1\right\}, 0\right\}\right)\alpha\beta MR}{(1+\alpha Z)^2}\right),
\end{aligned}
\right\} \tag{41}
$$

where $\Upsilon_i(t_f) = 0$, for $i = 1, 2, 3, \ldots, 9$ and $S(0) \geq 0$, $H(0) > 0$, $X(0) \geq 0$, $R(0) > 0$, $T(0) \geq 0$, $C(0) \geq 0$, $M(0) \geq 0$, $G(0) \geq 0$, $Z(0) > 0$.

Appendix C. Proof of Theorem 6

Let $(S, H, X, R, T, C, M, G, Z, \Upsilon_1, \Upsilon_2, \Upsilon_3, \Upsilon_4, \Upsilon_5, \Upsilon_6, \Upsilon_7, \Upsilon_8, \Upsilon_9)$ and $(\overline{X}, \overline{H}, \overline{S}, \overline{R}, \overline{T}, \overline{C}, \overline{M}, \overline{G}, \overline{Z}, \overline{\Upsilon}_1, \overline{\Upsilon}_2, \overline{\Upsilon}_3, \overline{\Upsilon}_4, \overline{\Upsilon}_5, \overline{\Upsilon}_6, \overline{\Upsilon}_7, \overline{\Upsilon}_8, \overline{\Upsilon}_9)$ be two different solutions of our optimality system (1) and (12). Suppose $S = e^{\Upsilon t}v_1$, $H = e^{\Upsilon t}v_2$, $X = e^{\Upsilon t}v_3$, $R = e^{\Upsilon t}v_4$, $T = e^{\Upsilon t}v_5$, $C = e^{\Upsilon t}v_6$, $M = e^{\Upsilon t}v_7$, $G = e^{\Upsilon t}v_8$, $Z = e^{\Upsilon t}v_9$, $\Upsilon_1 = e^{-\Upsilon t}w_1$, $\Upsilon_2 = e^{-\Upsilon t}w_2$, $\Upsilon_3 = e^{-\Upsilon t}w_3$, $\Upsilon_4 = e^{-\Upsilon t}w_4$, $\Upsilon_5 = e^{-\Upsilon t}w_5$, $\Upsilon_6 = e^{-\Upsilon t}w_6$, $\Upsilon_7 = e^{-\Upsilon t}$ $_7$, $\Upsilon_8 = e^{-\Upsilon t}w_8$ and $\Upsilon_9 = e^{-\Upsilon t}w_9$. Similarly, let $\overline{S} = e^{\Upsilon t}\overline{v}_1$, $\overline{H} = e^{\Upsilon t}\overline{v}_2$, $\overline{X} = e^{\Upsilon t}\overline{v}_3$, $\overline{R} = e^{\Upsilon t}\overline{v}_4$, $\overline{T} = e^{\Upsilon t}\overline{v}_5$, $\overline{C} = e^{\Upsilon t}\overline{v}_6$, $\overline{M} = e^{\Upsilon t}\overline{v}_7$, $\overline{G} = e^{\Upsilon t}\overline{v}_8$, $\overline{Z} = e^{\Upsilon t}\overline{v}_9$, $\overline{\Upsilon}_1 = e^{-\Upsilon t}\overline{w}_1$, $\overline{\Upsilon}_2 = e^{-\Upsilon t}\overline{w}_2$, $\overline{\Upsilon}_3 = e^{-\Upsilon t}\overline{w}_3$, $\overline{\Upsilon}_4 = e^{-\Upsilon t}\overline{w}_4$, $\overline{\Upsilon}_5 = e^{-\Upsilon t}\overline{w}_5$, $\overline{\Upsilon}_6 = e^{-\Upsilon t}\overline{w}_6$, $\overline{\Upsilon}_7 = e^{-\Upsilon t}\overline{w}_7$, $\overline{\Upsilon}_8 = e^{-\Upsilon t}\overline{w}_8$ and $\overline{\Upsilon}_9 = e^{-\Upsilon t}\overline{w}_9$. Further, we let

$$u_1^*(t) = \max\{\min\{(\beta_s(w_3 - w_2)v_1v_2e^{\Upsilon t})/B_1, 1\}, 0\},$$
$$\overline{u}_1^*(t) = \max\{\min\{(\beta_s(\overline{w}_3 - \overline{w}_2)\overline{v}_1\overline{v}_2e^{\Upsilon t})/B_1, 1\}, 0\} \quad \text{and}$$

$$|u_1^*(t) - \overline{u}_1^*(t)| \leq \frac{e^{\Upsilon t}\beta_s}{B_1}|((w_3 - w_2)v_1v_2 - (\overline{w}_3 - \overline{w}_2)\overline{v}_1\overline{v}_2)|; \tag{42}$$

$$u_2^*(t) = \max\left\{\min\left\{\frac{\beta_r(w_5 - w_4)v_5v_4e^{\Upsilon t}}{(1 + \alpha e^{\Upsilon t}v_9)B_2}, 1\right\}, 0\right\},$$
$$\overline{u}_2^*(t) = \max\left\{\min\left\{\frac{\beta_r(\overline{w}_5 - \overline{w}_4)\overline{v}_5\overline{v}_4e^{\Upsilon t}}{(1 + \alpha e^{\Upsilon t}\overline{v}_9)B_2}, 1\right\}, 0\right\} \quad \text{and}$$

$$|u_2^*(t) - \overline{u}_2^*(t)| \leq \frac{e^{\Upsilon t}\beta_r}{B_2}|\frac{(w_5 - w_4)v_5v_4(1 + \alpha e^{\Upsilon t}\overline{v}_9) - (\overline{w}_5 - \overline{w}_4)\overline{v}_5\overline{v}_4(1 + \alpha e^{\Upsilon t}v_9)}{(1 + \alpha e^{\Upsilon t}v_9)(1 + \alpha e^{\Upsilon t}\overline{v}_9)}|; \tag{43}$$

$$u_3^*(t) = \max\left\{\min\left\{\frac{w_8v_8 + w_7v_3\mu_xN}{B_3}, 1\right\}, 0\right\},$$
$$\overline{u}_3^*(t) = \max\left\{\min\left\{\frac{\overline{w}_8\overline{v}_8 + \overline{w}_7\overline{v}_3\mu_xN}{B_3}, 1\right\}, 0\right\}$$

and

$$|u_3^*(t) - \overline{u}_3^*(t)| \leq \frac{1}{B_3}|(w_8v_8 - \overline{w}_8\overline{v}_8) + \mu_xN(w_7v_3 - \overline{w}_7\overline{v}_3)|; \tag{44}$$

$$u_4^*(t) = \max\left\{\min\left\{\frac{w_7\mu_c(1 - \pi)Pv_6}{(1 + \alpha e^{\Upsilon t}v_9)B_4}, 1\right\}, 0\right\},$$
$$\overline{u}_4^*(t) = \max\left\{\min\left\{\frac{\overline{w}_7\mu_c(1 - \pi)P\overline{v}_6}{(1 + \alpha e^{\Upsilon t}\overline{v}_9)B_4}, 1\right\}, 0\right\}$$

and

$$|u_4^*(t) - \overline{u}_4^*(t)| \leq \frac{\mu_c(1 - \pi)P}{B_4}|\frac{w_7v_6(1 + \alpha e^{\Upsilon t}\overline{v}_9) - \overline{w}_7\overline{v}_6(1 + \alpha e^{\Upsilon t}v_9)}{(1 + \alpha e^{\Upsilon t}v_9)(1 + \alpha e^{\Upsilon t}\overline{v}_9)}|. \tag{45}$$

Substituting $S = e^{\Upsilon t}v_1$ into the first equation of system (1), (dS/dt), the state equation becomes

$$e^{\Upsilon t}(\dot{v}_1 + \Upsilon v_1) = \Upsilon - \mu_s v_1 e^{\Upsilon t} - \beta_s v_2 v_1 e^{2\lambda t}. \tag{46}$$

Similarly, substituting $\Upsilon_1 = e^{-\Upsilon t}w_1$ into the first equation of system (18), ($d\Upsilon_1/dt$), the adjoint equation becomes

$$e^{-\Upsilon t}(\dot{w}_1 - \Upsilon w_1) = (w_2 - w_3)(1 - u_1^*(t))\beta_s v_2 + \mu_s w_1 e^{-\Upsilon t} + \beta_s w_1 v_2. \tag{47}$$

Now, subtracting the equations for S and $\overline{S}$ in equation (46), Υ_1 and $\overline{\Upsilon}_1$ in equation (47) gives

$$\Upsilon(v_1 - \overline{v}_1) + (\dot{v}_1 - \dot{\overline{v}}_1) = -\mu_s(v_1 - \overline{v}_1) - \beta_s e^{\Upsilon t}(v_1v_2 - \overline{v}_1\overline{v}_2) \quad \text{and} \tag{48}$$

$$\Upsilon(w_1 - \overline{w}_1) + (\dot{w}_1 - \dot{\overline{w}}_1) = (1 - u_1^*)\beta_s e^{\Upsilon t}\{v_2(w_2 - w_3) - \overline{v}_2(\overline{w}_2 - \overline{w}_3)\} + \mu_s(w_1 - w_1) + \beta_s e^{\Upsilon t}(w_1v_2 - \overline{w}_1\overline{v}_2). \tag{49}$$

Multiplying each equation by appropriate difference of functions ($(v_1 - \overline{v}_1)$ and $(w_1 - \overline{w}_1)$, respectively) and integrating from 0 to t_f yields (for the case of equation (48))

$$\frac{1}{2}(v_1 - \overline{v}_1)^2 + \Upsilon\int_0^{t_f}(v_1 - \overline{v}_1)^2dt = -\mu_s\int_0^{t_f}(v_1 - \overline{v}_1)^2dt - \beta_s e^{\Upsilon t}\int_0^{t_f}(v_1v_2 - \overline{v}_1\overline{v}_2)(v_1 - \overline{v}_1)dt. \tag{50}$$

Applying the above procedure on the rest of the state and adjoint variables, we obtain

$$\frac{1}{2}(v_2-\bar{v}_2)^2+\Upsilon\int_0^{t_f}(v_2-\bar{v}_2)^2dt=-\mu_h\int_0^{t_f}(v_2-\bar{v}_2)^2dt-\beta_s\int_0^{t_f}(1-u_1^*)(v_1v_2-\bar{v}_1\bar{v}_2)(v_2-\bar{v}_2)e^{\Upsilon t}dt, \tag{51}$$

$$\begin{aligned}\frac{1}{2}(v_3-\bar{v}_3)^2+\Upsilon\int_0^{t_f}(v_3-\bar{v}_3)^2dt=&-\mu_x\int_0^{t_f}(v_3-\bar{v}_3)^2dt+\beta_s\int_0^{t_f}(1-u_1^*)(v_1v_2-\bar{v}_1\bar{v}_2)(v_3-\bar{v}_3)e^{\Upsilon t}dt\\&-k_x\int_0^{t_f}\left(\frac{v_3v_9}{1+\varepsilon_0e^{\Upsilon t}v_3}-\frac{\bar{v}_3\bar{v}_9}{1+\varepsilon_0e^{\Upsilon t}\bar{v}_3}\right)(v_3-\bar{v}_3)e^{\Upsilon t}dt,\end{aligned} \tag{52}$$

$$\frac{1}{2}(v_4-\bar{v}_4)^2+\Upsilon\int_0^{t_f}(v_4-\bar{v}_4)^2\,dt=-\beta_r\int_0^{t_f}(1-u_2^*)\left(\frac{v_4v_7}{1+\alpha e^{\Upsilon t}v_9}-\frac{\bar{v}_4\bar{v}_7}{1+\alpha e^{\Upsilon t}\bar{v}_9}\right)(v_4-\bar{v}_4)e^{\Upsilon t}dt-\mu_r\int_0^{t_f}(v_4-\bar{v}_4)^2\,dt, \tag{53}$$

$$\begin{aligned}\frac{1}{2}(v_5-\bar{v}_5)^2+\Upsilon\int_0^{t_f}(v_5-\bar{v}_5)^2dt=&\beta_r\int_0^{t_f}(1-u_2^*)\left(\frac{v_4v_7}{1+\alpha e^{\Upsilon t}v_9}-\frac{\bar{v}_4\bar{v}_7}{1+\alpha e^{\Upsilon t}\bar{v}_9}\right)(v_5-\bar{v}_5)e^{\Upsilon t}\,dt\\&-k_t\int_0^{t_f}\left(\frac{v_5v_9}{1+\varepsilon_1e^{\Upsilon t}v_5}-\frac{\bar{v}_5\bar{v}_9}{1+\varepsilon_1e^{\Upsilon t}\bar{v}_5}\right)(v_5-\bar{v}_5)e^{\Upsilon t}\,dt-(\mu_t+\gamma)\int_0^{t_f}(v_5-\bar{v}_5)^2\,dt,\end{aligned} \tag{54}$$

$$\begin{aligned}\frac{1}{2}(v_6-\bar{v}_6)^2+\Upsilon\int_0^{t_f}(v_6-\bar{v}_6)^2dt=&\gamma\int_0^{t_f}(v_5-\bar{v}_5)(v_6-\bar{v}_6)\,dt-\mu_c\int_0^{t_f}(v_6-\bar{v}_6)^2\,dt\\&-k_c\int_0^{t_f}\left(\frac{v_6v_9}{1+\varepsilon_2e^{\Upsilon t}v_6}-\frac{\bar{v}_6\bar{v}_9}{1+\varepsilon_2e^{\Upsilon t}\bar{v}_6}\right)(v_6-\bar{v}_6)e^{\Upsilon t}\,dt,\end{aligned} \tag{55}$$

$$\begin{aligned}\frac{1}{2}(v_7-\bar{v}_7)^2+\Upsilon\int_0^{t_f}(v_7-\bar{v}_7)^2dt=&\mu_xN\int_0^{t_f}(1-u_3^*)(v_3-\bar{v}_3)(v_7-\bar{v}_7)dt-(1-\pi)P\mu_c\int_0^{t_f}(1-u_4^*)\left(\frac{v_6}{1+\alpha e^{\Upsilon t}v_9}-\frac{\bar{v}_6}{1+\alpha e^{\Upsilon t}\bar{v}_9}\right)(v_7-\bar{v}_7)dt\\&-\mu_m\int_0^{t_f}(v_7-\bar{v}_7)dt-\beta_r\int_0^{t_f}(v_4v_7-\bar{v}_4\bar{v}_7)(v_7-\bar{v}_7)dt,\end{aligned} \tag{56}$$

$$\frac{1}{2}(v_8-\bar{v}_8)^2+\Upsilon\int_0^{t_f}(v_8-\bar{v}_8)^2dt=\pi\mu_c\int_0^{t_f}(v_6-\bar{v}_6)(v_8-\bar{v}_8)\,dt-\int_0^{t_f}(u_3^*-\mu_g)(v_8-\bar{v}_8)^2\,dt, \tag{57}$$

$$\begin{aligned}\frac{1}{2}(v_9-\bar{v}_9)^2+\Upsilon\int_0^{t_f}(v_9-\bar{v}_9)^2dt=&\delta_x\int_0^{t_f}\left(\frac{v_3}{1+\varepsilon_0e^{\Upsilon t}v_3}-\frac{\bar{v}_3}{1+\varepsilon_0e^{\Upsilon t}\bar{v}_3}\right)(v_9-\bar{v}_9)e^{\Upsilon t}dt\delta_t\int_0^{t_f}\left(\frac{v_5}{1+\varepsilon_1e^{\Upsilon t}v_5}-\frac{\bar{v}_5}{1+\varepsilon_1e^{\Upsilon t}\bar{v}_5}\right)(v_9-\bar{v}_9)e^{\Upsilon t}\\&dt\delta_c\int_0^{t_f}\left(\frac{v_6}{1+\varepsilon_2e^{\Upsilon t}v_6}-\frac{\bar{v}_6}{1+\varepsilon_2e^{\Upsilon t}\bar{v}_6}\right)(v_9-\bar{v}_9)e^{\Upsilon t}dt-\mu_z\int_0^{t_f}(v_9-\bar{v}_9)^2dt.\end{aligned} \tag{58}$$

Note that

$$(i)\quad k_x\int_0^{t_f}\left(\frac{v_3v_9}{1+\varepsilon_0e^{\Upsilon t}v_3}-\frac{\overline{v}_3\overline{v}_9}{1+\varepsilon_0e^{\Upsilon t}\overline{v}_3}\right)(v_3-\overline{v}_3)e^{\Upsilon t}\,dt = k_x\int_0^{t_f}\left(\frac{v_3v_9-\overline{v}_3\overline{v}_9}{(1+\varepsilon_0e^{\Upsilon t}v_3)(1+\varepsilon_0e^{\Upsilon t}\overline{v}_3}\right)(v_3-\overline{v}_3)e^{\Upsilon t}\,dt$$
$$+\varepsilon_0k_x\int_0^{t_f}\left(\frac{v_3v_9\overline{v}_3-\overline{v}_3\overline{v}_9v_3}{(1+\varepsilon_0e^{\Upsilon t}v_3)(1+\varepsilon_0e^{\Upsilon t}\overline{v}_3}\right)(v_3-\overline{v}_3)e^{2\Upsilon t}\,dt$$
$$\le (C_1e^{\Upsilon t_f}+C_2e^{2\Upsilon t_f})\int_0^{t_f}[(v_3-\overline{v}_3)^2+(v_9-\overline{v}_9)^2]\,dt \tag{59}$$

and

$$(ii)\quad \beta_s\int_0^{t_f}(1-u^*)(v_1v_2-\overline{v}_1\overline{v}_2)(v_3-\overline{v}_3)\,dt \le C_3e^{\Upsilon t_f}\int_0^{t_f}[(v_1-\overline{v}_1)^2+(v_2-\overline{v}_2)^2+(v_3-\overline{v}_3)^2]\,dt. \tag{60}$$

Upon combining the integrals in equations (50)-(58) gives

$$\begin{aligned}
&\frac{1}{2}(v_1-\overline{v}_1)^2(t_f)+\frac{1}{2}(v_2-\overline{v}_2)^2(t_f)+\frac{1}{2}(v_3-\overline{v}_3)^2(t_f)+\frac{1}{2}(v_4-\overline{v}_4)^2(t_f)+\frac{1}{2}(v_5-\overline{v}_5)^2(t_f)\\
&+\frac{1}{2}(v_6-\overline{v}_6)^2(t_f)+\frac{1}{2}(v_7-\overline{v}_7)^2(t_f)+\frac{1}{2}(v_8-\overline{v}_8)^2(t_f)+\frac{1}{2}(v_9-\overline{v}_9)^2(t_f)\\
&+\frac{1}{2}(w_1-\overline{w}_1)^2(0)+\frac{1}{2}(w_2-\overline{w}_2)^2(0)+\frac{1}{2}(w_3-\overline{w}_3)^2(0)+\frac{1}{2}(w_4-\overline{w}_4)^2(0)\\
&+\frac{1}{2}(w_5-\overline{w}_5)^2(0)+\frac{1}{2}(w_6-\overline{w}_6)^2(0)+\frac{1}{2}(w_7-\overline{w}_7)^2(0)+\frac{1}{2}(w_8-\overline{w}_8)^2(0)\\
&+\frac{1}{2}(w_9-\overline{w}_9)^2(0)+\Upsilon\int_0^{t_f}\Big[(v_1-v_1)^2+(v_2-v_2)^2+(v_3-v_3)^2+(v_4-v_4)^2\\
&+(v_5-v_5)^2+(v_6-v_6)^2+(v_7-v_7)^2+(v_8-v_8)^2+(v_9-v_9)^2+(w_1-w_1)^2\\
&+(w_2-w_2)^2+(w_3-w_3)^2+(w_4-w_4)^2+(w_5-w_5)^2+(w_6-w_6)^2\\
&+(w_7-w_7)^2+(w_8-w_8)^2+(w_9-w_9)^2\Big]\,dt
\end{aligned} \tag{61}$$

$$\begin{aligned}
&\le(\Upsilon-\overline{D}_1-\overline{D}_2e^{3\Upsilon t_f})\times\Big\{\int_0^{t_f}\Big[(v_1-v_1)^2+(v_2-v_2)^2+(v_3-v_3)^2+(v_4-v_4)^2+(v_5-v_5)^2+(v_6-v_6)^2\\
&+(v_7-v_7)^2+(v_8-v_8)^2+(v_9-v_9)^2\Big]+\int_0^{t_f}\Big[(w_1-w_1)^2+(w_2-w_2)^2\\
&+(w_3-w_3)^2+(w_4-w_4)^2+(w_5-w_5)^2+(w_6-w_6)^2+(w_7-w_7)^2+(w_8-w_8)^2+(w_9-w_9)^2\Big]\Big\},
\end{aligned} \tag{62}$$

where $\overline{D}_1$ and $\overline{D}_2$ depend on the coefficients and the bounds of v_i and w_i, $i=1,\ldots,9$. If Υ is chosen such that $\Upsilon>\overline{D}_1+\overline{D}_2$ and $t_f<\frac{1}{3\Upsilon}\ln\left(\frac{\Upsilon-\overline{D}_1}{\overline{D}_2}\right)$, then $v_1=\overline{v}_1, v_2=\overline{v}_2, v_3=\overline{v}_3, v_4=\overline{v}_4, v_5=\overline{v}_5, v_6=\overline{v}_6, v_7=\overline{v}_7, v_8=\overline{v}_8, v_9=\overline{v}_9, w_1=\overline{w}_1, w_2=\overline{w}_2, w_3=\overline{w}_3, w_4=\overline{w}_4, w_5=\overline{w}_5, w_6=\overline{w}_6, w_7=\overline{w}_7, w_8=\overline{w}_8, w_9=\overline{w}_9$. This shows that the solution to the optimality system (1) and (12) is unique.

References

Abdulla, S., Agre, P., Alonso, P., Arevalo-Herrera, M., Bassat, Q., Binka, F., et al. (2011). A research agenda for malaria eradication: Vaccines. *PLoS One, 8*(1), Article e1000398. https://doi.org/10.1371/journal.pmed.1000398

Aguilar, J. B., & Gutierrez, J. B. (2020). An epidemiological model of malaria accounting for asymptomatic carriers. *Bulletin of Mathematical Biology, 82*(3), 1–55.

Agusto, F. B., Marcus, N., & Okosun, K. O. (2012). Application of optimal control to the epidemiology of malaria. *Bulletin of mathematical biology 2012*, (81), 1–22.

Al-Awadhi, M., Ahmad, S., & Iqbal, J. (2021). Current status and the epidemiology of malaria in the middle east region and beyond. *Microorganisms 2021, 9*, 338'.
Anderson, R., May, R., & Gupta, S. (1989). Non-linear phenomena in-host parasite interactions. *Parasitology, 99*(S1), S59–S79.
Anita, S., Capasso, V., & Arnautu, V. (2011). *An introduction to optimal control problems in life Sciences and economics: From mathematical models to numerical simulation with MATLAB®*. Springer.
Arya, A., Foko, L. P. K., Chaudhry, S., & Singh, V. (2020). Artemisinin-based combination therapy (act) and drug resistance molecular markers: A systematic review of clinical studies from two malaria endemic regions—India and sub saharan africa. *International Journal for Parasitology: Drugs and Drug Resistance, 15*, 43–56.
Bauza, K., Atcheson, E., Malinauskas, T., Blagborough, A. M., & Reyes-Sandoval, A. (2016). Tailoring a combination preerythrocytic malaria vaccine. *Infection and Immunity, 84*(3), 622–634.
Birkett, A. J. (2016). Status of vaccine research and development of vaccines for malaria. *Vaccine, 34*(26), 2915–2920.
Caveny, J. (1970). On integral lipschitz conditions and integral bounded variation. *Journal of the London Mathematical Society, 2*(2), 346–352.
CDC. (2017). *Malaria biology*. Technical report. Center for Disease Control and Prevention. Center for Disease Control. Retrieved from https://www.cdc.gov/malaria/about/biology/. January 2017.
Chitnis, C. E., Mukherjee, P., Mehta, S., Yazdani, S. S., Dhawan, S., Shakri, A. R., et al. (2015). Phase I clinical trial of a recombinant blood stage vaccine candidate for plasmodium falciparum malaria based on MSP1 and EBA175. *PLoS One, 10*(4), Article e0117820. https://doi.org/10.1371/journal.pone.0117820
Chiyaka, C. (2010). Using mathematics to understand malaria infection during erythrocytic stages. *Zimbabwe journal of science and technology, 5*, 1–11, 2010.
Chiyaka, C., Garira, W., & Dube, S. (2008). Modelling immune response and drug therapy in human malaria infection. *Computational and Mathematical Methods in Medicine, 9*(2), 143–163.
Chuma, F., Mwanga, G. G., & Masanja, V. G. (2019). Application of optimal control theory to newcastle disease dynamics in village chicken by considering wild birds as reservoir of disease virus. *Journal of Applied Mathematics, 2019*, 14. https://doi.org/10.1155/2019/3024965. Article ID 3024965.
Cowman, A. F., Berry, D., & Baum, J. (2012). The cellular and molecular basis for malaria parasite invasion of the human red blood cell. *The Journal of Cell Biology, 198*(6), 961–971.
Diebner, H. H., Eichner, M., Molineaux, L., Collins, W. E., Jeffery, G. M., & Dietz, K. (2000). Modelling the transition of asexual blood stages of plasmodium falciparum to gametocytes. *Journal of Theoretical Biology, 202*(2), 113–127.
Dondorp, A. M., Kager, P. A., Vreeken, J., & White, N. J. (2000). Abnormal blood flow and red blood cell deformability in severe malaria. *Parasitology Today, 16*(6), 228–232.
Dondorp, A. M., Nosten, F., Yi, P., Das, D., Phyo, A. P., Tarning, J., et al. (2009). Artemisinin resistance in plasmodium falciparum malaria. *New England Journal of Medicine, 361*(5), 455–467.
Duru, V., Witkowski, B., & Ménard, D. (2016). Plasmodium falciparum resistance to artemisinin derivatives and piperaquine: A major challenge for malaria elimination in Cambodia. *The American Journal of Tropical Medicine and Hygiene, 95*(6), 1228–1238.
Eziefula, A. C., Bousema, T., Yeung, S., Kamya, M., Owaraganise, A., Gabagaya, G., et al. (2014). Single dose primaquine for clearance of plasmodium falciparum gametocytes in children with uncomplicated malaria in Uganda: A randomised, controlled, double-blind, dose-ranging trial. *The Lancet Infectious Diseases, 14*(2), 130–139.
Fleming, W., & Rishel, R. (1975). *Optimal Deterministic and stochastic control, applications of mathematics*. Berlin, Germany: Springer.
Gaff, H., & Schaefer, E. (2009). Optimal control applied to vaccination and treatment strategies for various epidemiological models. *Mathematical Biosciences and Engineering: MBE, 6*(3), 469–492.
Garrett, B., & Rota, G.-C. (1978). *Ordinary differential equations* (3rd ed.). New York: John Wiley and Sons.
Hodel, E. M., Kay, K., & Hastings, I. M. (2016). Incorporating stage-specific drug action into pharmacological modeling of antimalarial drug treatment. *Antimicrobial Agents and Chemotherapy, 60*(5), 2747–2756.
Iman, R. L., & Helton, J. C. (1988). An investigation of uncertainty and sensitivity analysis techniques for computer models. *Risk Analysis, 8*(1), 71–90.
Ince, E. L. (1943). *Integration of ordinary differential equations*. Oliver and Boyd: University mathematical texts. https://books.google.de/books?id=SBVOAQAAIAAJ.
Iooss, B., & Saltelli, A. (2017). Introduction to sensitivity analysis. In R. Ghanem, D. Higdon, & H. Owhadi (Eds.), *Handbook of uncertainty quantification*. Cham: Springer.
Joshi, H. R., Lenhart, S., Li, M. Y., & Wang, L. (2006). Optimal control methods applied to disease models. *Contemporary Mathematics, 410*, 187–208.
Kamgang, J. C., & Sallet, G. (2005). Global asymptotic stability for the disease free equilibrium for epidemiological models. *Comptes Rendus Mathematique, 341*(7), 433–438.
Kim, B. N., Nah, K., Chu, C., Ryu, S. U., Kang, Y. H., & Kim, Y. (2012). Optimal control strategy of plasmodium vivax malaria transmission in korea. *Osong Public Health and Research Perspectives, 3*(3), 128–136.
Kioko, U., Riley, C., Dellicour, S., Were, V., Ouma, P., Gutman, J., et al. (2016). A cross-sectional study of the availability and price of anti-malarial medicines and malaria rapid diagnostic tests in private sector retail drug outlets in rural western Kenya, 2013. *Malaria Journal, 15*(359). https://doi.org/10.1186/s12936-016-1404-5
Lashari, A. A., Hattaf, K., Zaman, G., & Li, X.-Z. (2013). Backward bifurcation and optimal control of a vector borne disease. *Applied Mathematics & Information Sciences, 7*(1), 301–309.
Lenhart, S., & Workman, J. T. (2007). *Optimal control applied to biological models*. USA: Chapman and Hall/CRC.
Li, Y., Ruan, S., & Xiao, D. (2011). The within-host dynamics of malaria infection with immune response. *Mathematical Biosciences and Engineering, 8*(4), 999–1018.
MA. (2019). *'Antimalarial drugs', Malaria site*. Retrieved from https://www.malariasite.com/malaria-drugs/. March, 2019.
Magombedze, G., Chiyaka, C., & Mukandavire, Z. (2011). Optimal control of malaria chemotherapy. *Nonlinear Analysis Modelling and Control, 16*(4), 415–434.
Mahmoudi, S., & Keshavarz, H. (2018). Malaria vaccine development: The need for novel approaches: A review article. *Iranian Journal of Parasitology, 13*(1), 1–10.
Mairet-Khedim, M., Leang, R., Marmai, C., Khim, N., Kim, S., Ke, S., et al. (2020). Clinical and in vitro resistance of plasmodium falciparum to artesunate-amodiaquine in Cambodia. *Clinical Infectious Diseases*.
Makinde, O. D., & Okosun, K. O. (2011). Impact of chemo-therapy on optimal control of malaria disease with infected immigrants. *Biosystems, 104*(1), 32–41.
Miura, K. (2016). Progress and prospects for blood-stage malaria vaccines. *Expert Review of Vaccines, 15*(6), 765–781.
Mlay, G. M., Luboobi, L., Kuznetsov, D., & Shahada, F. (2015). Optimal treatment and vaccination control strategies for the dynamics of pulmonary tuberculosis. *International Journal of Advances in Applied Mathematics and Mechanics, 2*(3), 196–207.
Molineaux, L., & Dietz, K. (1999). Review of intra-host models of malaria. *Parassitologia, 41*(1), 221–232.
Mombo-Ngoma, G., Remppis, J., Sievers, M., Zoleko Manego, R., Endamne, L., Kabwende, L., et al. (2017). Efficacy and safety of fosmidomycin—piperaquine as nonartemisinin-based combination therapy for uncomplicated falciparum malaria: A single-arm, age de-escalation proof-of-concept study in Gabon. *Clinical Infectious Diseases, 66*(12), 1823–1830.
Mpeshe, S. C., Luboobi, L. S., & Nkansah-gyekye, Y. (2014). Optimal control strategies for the dynamics of Rift Valley fever. *Communications in Optimization Theory, 26*(3), 385–402.
Mwanga, G. G., Haario, H., & Capasso, V. (2015). Optimal control problems of epidemic systems with parameter uncertainties: Application to a malaria two-age-classes transmission model with asymptomatic carriers. *Mathematical Biosciences, 261*, 1–12.
Mwanga, G. G., Haario, H., & Nannyonga, B. (2014). Optimal control of malaria model with drug resistance in presence of parameter uncertainty. *Applied Mathematical Sciences, 8*(55), 2701–2730.

Nakakawa, J., Mugisha, J. Y., Shaw, M. W., Tinzaara, W., & Karamura, E. (2017). Banana xanthomonas wilt infection: The role of debudding and roguing as control options within a mixed cultivar plantation. *International Journal of Mathematics and Mathematical Sciences*, 13. https://doi.org/10.1155/2017/4865015, 2017, Article ID 4865015.
Namawejje, H., Luboobi, L. S., Kuznetsov, D., & Wobudeya, E. (2014). Modeling optimal control of rotavirus disease with different control strategies. *Journal of Mathematical and Computational Science, 4*(5), 892–914.
NIH. (2019). *Clinical Trials*. US National Library of Medicine. Retrieved from https://clinicaltrials.gov/ct2/results?cond=Malaria%2CFalciparum&term=vaccine+combinations&cntry=&state=&city=&dist=. (Accessed April 2019).
Noedl, H., Se, Y., Schaecher, K., Smith, B. L., Socheat, D., & Fukuda, M. M. (2008). Evidence of artemisinin-resistant malaria in western Cambodia. *New England Journal of Medicine, 359*(24), 2619–2620.
Ogutu, B. (2013). Artemether and lumefantrine for the treatment of uncomplicated plasmodium falciparum malaria in sub-saharan africa. *Expert Opinion on Pharmacotherapy, 14*(5), 643–654.
Ogutu, B. R., Apollo, O. J., McKinney, D., Okoth, W., Siangla, J., Dubovsky, F., et al. (2009). Blood stage malaria vaccine eliciting high antigen-specific antibody concentrations confers no protection to young children in Western Kenya. *PLoS One, 4*(3), Article e4708. https://doi.org/10.1371/journal.pone.0004708
Okell, L. C., Drakeley, C. J., Bousema, T., Whitty, C. J., & Ghani, A. C. (2008). Modelling the impact of artemisinin combination therapy and long-acting treatments on malaria transmission intensity. *PLoS Medicine, 5*(11), e226. https://doi.org/10.1371/journal.pmed.0050226
Okosun, K. O., Ouifki, R., & Marcus, N. (2011). Optimal control analysis of a malaria disease transmission model that includes treatment and vaccination with waning immunity. *Biosystems, 106*(2–3), 136–145.
Omondi, E. O., Orwa, T. O., & Nyabadza, F. (2018). Application of optimal control to the onchocerciasis transmission model with treatment. *Mathematical Biosciences, 297*, 43–57.
Orwa, T. O., Mbogo, R. W., & Luboobi, L. S. (2018 a). Mathematical model for hepatocytic-erythrocytic dynamics of malaria. *International Journal of Mathematics and Mathematical Sciences 2018, 2018*. https://doi.org/10.1155/2018/7019868. Article ID 7019868, 18 pages.
Orwa, T. O., Mbogo, R. W., & Luboobi, L. S. (2018 b). Mathematical model for the in-host malaria dynamics subject to malaria vaccines. *Letters in Biomathematics, 5*(1), 222–251.
Orwa, T. O., Mbogo, R. W., & Luboobi, L. S. (2019 a). Multiple-strain malaria infection and its impacts on plasmodium falciparum resistance to antimalarial therapy: A mathematical modelling perspective. *Computational and Mathematical Methods in Medicine 2019, 2019*. https://doi.org/10.1155/2019/9783986. Article ID 9783986, 26 pages.
Orwa, T. O., Mbogo, R. W., & Luboobi, L. S. (2019 b). Uncertainty and sensitivity analysis applied to an in-host malaria model with multiple vaccine antigens. *International Journal of Applied and Computational Mathematics, 5*(3), 73. https://doi.org/10.1007/s40819-019-0658-3
Osorio, L., Gonzalez, I., Olliaro, P., & Taylor, W. R. (2007). Artemisinin-based combination therapy for uncomplicated *Plasmodium falciparum* malaria in Colombia. *Malaria Journal, 6*(25). https://doi.org/10.1186/1475-2875-6-25
Palafox, B., Patouillard, E., Tougher, S., Goodman, C., Hanson, K., Kleinschmidt, I., et al. (2015). Prices and mark-ups on antimalarials: Evidence from nationally representative studies in six malaria-endemic countries. *Health Policy and Planning, 31*(2), 148–160.
Penny, M. A., Verity, R., Bever, C. A., Sauboin, C., Galactionova, K., Flasche, S., et al. (2016). Public health impact and cost-effectiveness of the rts, s/as01 malaria vaccine: A systematic comparison of predictions from four mathematical models. *The Lancet, 387*(10016), 367–375.
Pukrittayakamee, S., Chotivanich, K., Chantra, A., Clemens, R., Looareesuwan, S., & White, N. J. (2004). Activities of artesunate and primaquine against asexual-and sexual-stage parasites in falciparum malaria. *Antimicrobial Agents and Chemotherapy, 48*(4), 1329–1334.
Selemani, M. A., Luboobi, L. S., & Nkansah-Gyekye, Y. (2016). On stability of the in-human host and in-mosquito dynamics of malaria parasite. *Asian Journal of Mathematics and Applications 2016*, 23–26. ISSN 2307-7743.
Sherrard-Smith, E., Sala, K. A., Betancourt, M., Upton, L. M., Angrisano, F., Morin, M. J., et al. (2018). Synergy in anti-malarial pre-erythrocytic and transmission-blocking antibodies is achieved by reducing parasite density. *Elife, 7*, Article e35213. https://doi.org/10.7554/eLife.35213
Silva, C. J., & Torres, D. F. (2013). An optimal control approach to malaria prevention via insecticide-treated nets. In *Conference papers in science* (Vol. 2013) Hindawi.
Smithuis, F., Kyaw, M. K., Phe, O., Win, T., Aung, P. P., Oo, A. P. P., et al. (2010). Effectiveness of five artemisinin combination regimens with or without primaquine in uncomplicated falciparum malaria: An open-label randomised trial. *The Lancet Infectious Diseases, 10*(10), 673–681.
Talman, A. M., Domarle, O., McKenzie, F. E., Ariey, F., & Robert, V. (2004). Gametocytogenesis: The puberty of plasmodium falciparum. *Malaria Journal, 3*(1), 24–35.
Tumwiine, J., Mugisha, J., & Luboobi, L. (2008). On global stability of the intra-host dynamics of malaria and the immune system. *Journal of Mathematical Analysis and Applications, 341*(2), 855–869.
Van den Driessche, P., & Watmough, J. (2002). Reproduction numbers and sub-threshold endemic equilibria for compartmental models of disease transmission. *Mathematical Biosciences, 180*(1), 29–48.
Visser, B. J., van Vugt, M., & Grobusch, M. P. (2014). Malaria: An update on current chemotherapy. *Expert Opinion on Pharmacotherapy, 15*(15), 2219–2254.
Wang, X. (2004). A simple proof of descartes's rule of signs. *The American Mathematical Monthly, 111*(6), 525. https://doi.org/10.2307/4145072
White, N. J., Qiao, L. G., Qi, G., & Luzzatto, L. (2012). Rationale for recommending a lower dose of primaquine as a plasmodium falciparum gametocytocide in populations where G6PD deficiency is common. *Malaria Journal, 11*(418). https://doi.org/10.1186/1475-2875-11-418
WHO. (2012). *Single dose primaquine as a gametocytocide in plasmodium falciparum malaria; updated WHO policy recommendation*. World Health Organization. Retrieved from https://www.who.int/malaria/publications/atoz/who_pq_policy_recommendation/en/. (Accessed April 2019).
WHO. (2015a). *Global technical strategy for malaria 2016-2030*. World Health Organization. Retrieved from https://apps.who.int/iris/bitstream/handle/10665/176712/9789241564991_eng.pdf?sequence=1. (Accessed June 2019).
WHO. (2015b). *Guidelines for the treatment of malaria. Third edition April 2015*. World Health Organization. Retrieved from https://www.who.int/malaria/publications/atoz/9789241549127/en/. (Accessed April 2019).
WHO. (2016). *World malaria report 2016*. World Health Organization. Retrieved from https://www.who.int/malaria/publications/world-malaria-report-2016/report/en/. (Accessed November 2018).
WHO. (2018). *Artemisinin resistance and artemisinin-based combination therapy efficacy: Status report*. Technical report. World Health Organization.
WHO. (2020). *World malaria report 2020*. World Health Organization. Retrieved from https://www.who.int/teams/global-malaria-programme/reports/world-malaria-report-2020. June 2021.
Winskill, P., Slater, H. C., Griffin, J. T., Ghani, A. C., & Walker, P. G. (2017a). The us president's malaria initiative, plasmodium falciparum transmission and mortality: A modelling study. *PLoS Medicine, 14*(11), Article e1002448. https://doi.org/10.1371/journal.pmed.1002448
Winskill, P., Walker, P. G., Griffin, J. T., & Ghani, A. C. (2017b). Modelling the cost-effectiveness of introducing the rts, s malaria vaccine relative to scaling up other malaria interventions in sub-Saharan Africa. *BMJ Global Health, 2*(1), Article e000090. https://doi.org/10.1136/bmjgh-2016-000090
Yiga, V., Nampala, H., & Tumwiine, J. (2020). Analysis of the model on the effect of seasonal factors on malaria transmission dynamics. *Journal of Applied Mathematics, 2020*, 19, 8885558.